

A multi observation analysis of the 2017 dense water formation events: climate change, bottom density currents and Adriatic-Ionian Sea circulation (Mediterranean Sea).

Riccardo Martellucci¹, Francesco Paladini de Mendoza², Milena Menna³, Annunziata Pirro³, Marco Reale³, Miroslav Gačić³, Pierre-Marie Poulain⁴, Francesco riminucci⁵, Le Meur Julien³, Patrizia Giordano², Leonardo Langone⁶, Vanessa R. Cardin⁷, Carolina Cantoni⁵, Caterina Bergami⁵, Federica Grilli⁸, Mauro Marini⁸, Antonella Gallo³, Giulio Notarstefano³, Simone Toller⁵, Mauro Bastianini⁵, Martina Kralj³, Tommaso Diociaiuti³, Massimo Pacciaroni³, Antonio Bussani³, Elena Mauri³, and Stefano Miserocchi⁹

¹National Institute of oceanography and Applied Geophysics, Italy

²National Research Council-Institute of Polar Sciences (CNR-ISP)

³National Institute of oceanography and Applied Geophysics

⁴CMRE

⁵National Research Council-Institute of Marine Sciences (CNR-ISMAR)

⁶Consiglio Nazionale delle Ricerche - Istituto di Scienze Polari

⁷Borgo Grotta Gigante 42/c

⁸National Research Council-Institute for Biological Resources and Marine Biotechnologies (CNR-IRBIM)

⁹CNR-ISP

January 11, 2025

Abstract

The Mediterranean Sea is a critical hotspot for climate and biodiversity, where dense water formation and its spreading significantly influence thermohaline circulation and biogeochemical exchanges. In this context, the Adriatic Observatory Network serves as a leading example of a basin-scale observatory to study ecosystem dynamics across the Adriatic and Ionian Seas, integrating different infrastructures and producing FAIR (Findable, Accessible, Interoperable, Reusable) data. This network has unveiled a previously unexplored aspect occurred in 2017, with potential impact on the Mediterranean basin scale circulation. In 2016-2017, the central Mediterranean experienced significant heat loss, reduced freshwater input, and a persistent cyclonic phase of the Northern Ionian Gyre, which drove salt water into the Adriatic. These conditions facilitated dense water formation in the northern and southern Adriatic by shelf and open-ocean convection. The dense water formed in the north flows southward along the western continental slope, in part cascading into the southern Adriatic Pit, where it mixes with resident waters to form the Adriatic deep water, which then spreads into the Ionian Sea. Our findings revealed that another part of the northern dense water flows directly towards the strait of Otranto without being further altered on the way. These two water masses follow two different fates after their outflow into the Ionian Sea: southward along the Hellenic Trench and westward towards the Gulf of Taranto, respectively. The westward flow contributes to the reversal of the Northern Ionian Gyre, while the southward sinking affects the deep layers of the Hellenic Trench and the Levantine Basin.

Hosted file

Supporting information.docx available at <https://authorea.com/users/877690/articles/1257104-a-multi-observation-analysis-of-the-2017-dense-water-formation-events-climate-change-bottom-density-currents-and-adriatic-ionic-sea-circulation-mediterranean-sea>

A multi observation analysis of the 2017 dense water formation events: climate change, bottom density currents and Adriatic-Ionian Sea circulation (Mediterranean Sea).

Martellucci R.^{†1}, Paladini de Mendoza F.^{†2}, Menna M.¹, Pirro A.¹, Reale¹, M., Gačić M.¹, Poulain P.M.³, Riminucci F.⁴, Le Meur J.¹, Giordano P.⁵, Langone L.⁵, Cardin V.¹, Cantoni C.⁶, Bergami C.⁴, Grilli F.⁷, Marini M.⁷, Gallo A.¹, Notarstefano G.¹, Toller S.⁴, Bastianini M.⁴, Krali M.¹, Diociaiuti T.¹, Pacciaroni M.¹, Bussani A.¹, Miserocchi S.⁵ & Mauri E.¹

† These authors contributed equally to this work

¹ National Institute of Oceanography and Applied Geophysics (OGS), Trieste, Italy.

² National Research Council-Institute of Polar Sciences (CNR-ISP), Messina, Italy.

³ Centre for Maritime Research and Experimentation (CMRE), La Spezia, Italy.

⁴ National Research Council-Institute of Marine Sciences (CNR-ISMAR), Venice, Italy.

⁵ National Research Council-Institute of Polar Sciences (CNR-ISP), Bologna, Italy.

⁶ National Research Council-Institute of Marine Sciences (CNR-ISMAR), Trieste, Italy.

⁷ National Research Council-Institute for Biological Resources and Marine Biotechnologies (CNR-IRBIM), Ancona, Italy.

rmartellucci@ogs.it

francesco.paladinidemendoza@cnr.it

Abstract

The Mediterranean Sea is a critical hotspot for climate and biodiversity, where dense water formation and its spreading significantly influence thermohaline circulation and biogeochemical exchanges. In this context, the Adriatic Observatory Network serves as a leading example of a basin-scale observatory to study ecosystem dynamics across the Adriatic and Ionian Seas, integrating different infrastructures and producing FAIR (Findable, Accessible, Interoperable, Reusable) data. This network has unveiled a previously unexplored aspect occurred in 2017, with potential impact on the Mediterranean basin scale circulation.

In 2016-2017, the central Mediterranean experienced significant heat loss, reduced freshwater input, and a persistent cyclonic phase of the Northern Ionian Gyre, which drove salt water into the Adriatic. These conditions facilitated dense water formation in the northern and southern Adriatic by shelf and open-ocean convection. The dense water formed in the north flows southward along the western continental slope, in part cascading into the southern Adriatic Pit, where it mixes with resident waters to form the Adriatic deep water, which then spreads into the Ionian Sea. Our findings revealed that another part of the northern dense water flows directly towards the strait of Otranto without being further altered on the way. These two water masses follow two different fates after their outflow into the Ionian Sea: southward along the Hellenic Trench and westward towards the Gulf of Taranto, respectively. The westward flow contributes to the reversal of the Northern Ionian Gyre, while the southward sinking affects the deep layers of the Hellenic Trench and the Levantine Basin.

Plain Language Summary

The Mediterranean is a crucial region for global climate and biodiversity. The dense water formed here plays a key role in ocean circulation and marine ecosystems. The Adriatic Sea serves as source of dense water, and thanks to the Adriatic Observatory Network, the basin has become a laboratory for monitoring oceanographic processes. The network is multidisciplinary and uses different oceanographic platforms and model products.

In the winter of 2016-2017, severe meteorological conditions led to the formation of dense water in the Adriatic Sea. This dense water moved southwards and mixed with the existing water, creating deep water in the southern Adriatic. This deep water then flowed through the Strait of Otranto into the eastern Mediterranean. For the first time, two distinct pathways of dense water outflow were clearly observed: one westward and another southward along the Hellenic Trench. These paths have different effects on the Ionian and influence the currents and deep-sea circulation patterns. The westerly current contributes to changes in the surface circulation of the Ionian, while the southerly current influences the abyssal plain of the eastern Mediterranean. This study demonstrates the importance of maintaining observing systems that provide FAIR data, which are crucial for understanding complex ocean processes.

Highlights:

Dense water produced in the Adriatic Sea is a significant oceanographic feature and key component of Mediterranean thermohaline circulation.

The observation network follows the dense water from its place of origin to its fate on its way into the deep Ionian Sea in 2017.

Argo floats in the northern Ionian Sea captured the signature of deep-water observing for the first time a double pathway of this water mass.

Introduction

The Mediterranean Sea is a mid-latitude semi-enclosed basin with limited exchanges with the open ocean, resulting in distinct, faster circulation patterns compared to the global ocean (Malanotte-Rizzoli et al., 2014) and rich dynamics over a wide range of interacting scales (Chiggiato et al., 2023). The heat absorbed at the surface layer can be transferred to the deep ocean in the areas where dense water (dW) forms (Kubin et al., 2023, Pirro et al., 2024) and/or through boundary currents and mesoscale eddies (Waldman et al., 2018; Kubin et al., 2019; Pinardi et al., 2019). These mechanisms have significant impact on the deep-water circulation and on ecosystem dynamics at the basin scale, playing a key role in the biogeochemical shelf-deep ocean exchanges (Ivanov et al., 2004; Pinardi et al., 2023; Vilibić et al., 2023).

The warming of the Mediterranean Sea can affect the stratification of the water column (Parras-Berrocal et al., 2022 and 2023; Josey & Schroeder, 2023), with an impact on dW formation and thermohaline circulation (Reale et al., 2022). Since 2013, the Gulf of Lions has witnessed the absence of deep convection (Coppola et al., 2018; Margirier et al., 2020; Bosse et al., 2021; Fourier et al., 2022; Josey & Schroeder, 2023; Durrieu de Madron et al., 2023), due to the reduction in winter heat

losses (Josey & Schroeder, 2023) and temperature and salinity increase of the intermediate water (Margirier et al., 2020).

The dW can be formed by open-ocean convection (Marshall & Scott, 1999; Houpert et al., 2016; Testor et al., 2018; Somot et al., 2018) and shelf convection (Bensi et al., 2013; Vilibić et al., 2023). Shelf convection occurs at coastal margins due to a combination of several factors affecting the thermohaline properties of the surface water and is mainly driven by heat losses that generate dW masses flowing downward in a near-vertical mixing due to their buoyancy properties (Shapiro et al., 2003).

In the Adriatic Sea (Figure 1), a semi-enclosed basin in the northeasternmost part of the Mediterranean Sea, both types of convection occur (Manca et al., 2002): (i) shelf convection in the northern Adriatic, producing the North Adriatic dense Water (NAddW, Vilibić et al., 2023, Schroeder et al., 2024) and (ii) open-ocean convection (Pirro et al., 2022) in the Southern Adriatic Pit (SAP).

The basin itself significantly influences the spreading of dW, starting with a relatively shallow northern shelves (maximum depth 40 m), continues into the central Pomo Pit (approximately 200 m deep) and ends in the greater depths of the SAP (approximately 1250 m). The southern edge of the Pit opens at about 800 m across the strait of Otranto (to a depth of 900 m; Figure 1d) towards the deeper Ionian Basin and allows the outflow of dW.

The formation of NAddW is driven by heat losses, limited freshwater input from the Po River, ocean circulation in the basin and inflow of saltier water (Shapiro et al., 2003, Raicich et al., 2013, Vilibić et al., 2023) from the Ionian Sea. This inflow is influenced by the decadal reversal of the Northern Ionian Gyre (NIG, Civitarese et al., 2023; Mihanović et al., 2021), which brings more/less saline water to the southern Adriatic during cyclonic/anticyclonic modes of the NIG (Menna et al., 2021). Events characterised by extremely dense NAddW occur almost cyclically and this phenomenon has been termed as "saw-tooth mechanism" (Querin et al., 2016).

During the winter season strong, dry and cold northeasterly winds trigger the formation of the dW in the northern Adriatic, which, once formed, flows southwards along the western side of the Adriatic basin, following the isobaths (Vilibić & Supić, 2005, Benetazzo et al., 2014). On their way, they partially cascade in the Pomo Pit (Marini et al., 2016, Vilibić et al., 2023, Le Meur et al., 2024) before reaching the shelf edge of the southern basin. Here, the dW mostly sinks along the western side of the continental slope, in particular along the Bari Canyon system (Turchetto et al., 2007; Langone et al., 2016). Moreover, a smaller part flows along the Italian shelf reaching the strait of Otranto (Bignami et al., 1990; Manca et al., 2002; Ursella et al., 2012; Rovere et al., 2019). Once the NAddW enters the Southern Adriatic Pit, it mixes with the surrounding waters and forms the Adriatic Deep Water (ADdW), which flows out through the strait of Otranto into the Ionian Sea and influences both the surface (Rubino et al., 2020, Gačić et al., 2021) and the deep-circulation of the eastern Mediterranean Sea (Manca et al., 2006). This can significantly impact the entire circulation of the Mediterranean Sea (Menna et al., 2019, 2021, 2022).

Along its path, the thermohaline characteristics of the dW exhibit notable changes and the range of variation strictly depends on the variability of the drivers (Sellschopp & Alvarez, 2003). For example, during the extreme event in winter 2012 (Bensi et al., 2013; Chiggiato et al., 2016), strong heat losses ($>200 \text{ W m}^{-2}$, Vilibić et al., 2023) and a significant increase in the salinity resulted in a potential density anomaly (σ_θ) for the dW $> 30 \text{ kg m}^{-3}$.

126 The complex mechanisms driving the formation and dynamics of NAddW span multiple temporal
127 and spatial scales, necessitating detailed analysis supported by high-resolution observational and
128 numerical tools. In this context the multi-platform observing system analysis proved essential for
129 unraveling complex dynamic processes across spatio-temporal scales that cannot be resolved using
130 a single-platform approach alone. (Berta et al., 2018; Martellucci et al., 2021).
131 Here, taking advantage of the Adriatic Observatory Network we have analysed the dynamics of the
132 NAddW from its formation area to its fate on the way to the deep Ionian Sea during a particularly
133 intense dW formation event that occurred in winter 2017, exploiting for the first time the full
134 potential of the observational network developed in the Adriatic-Ionian region since the late 1990s.

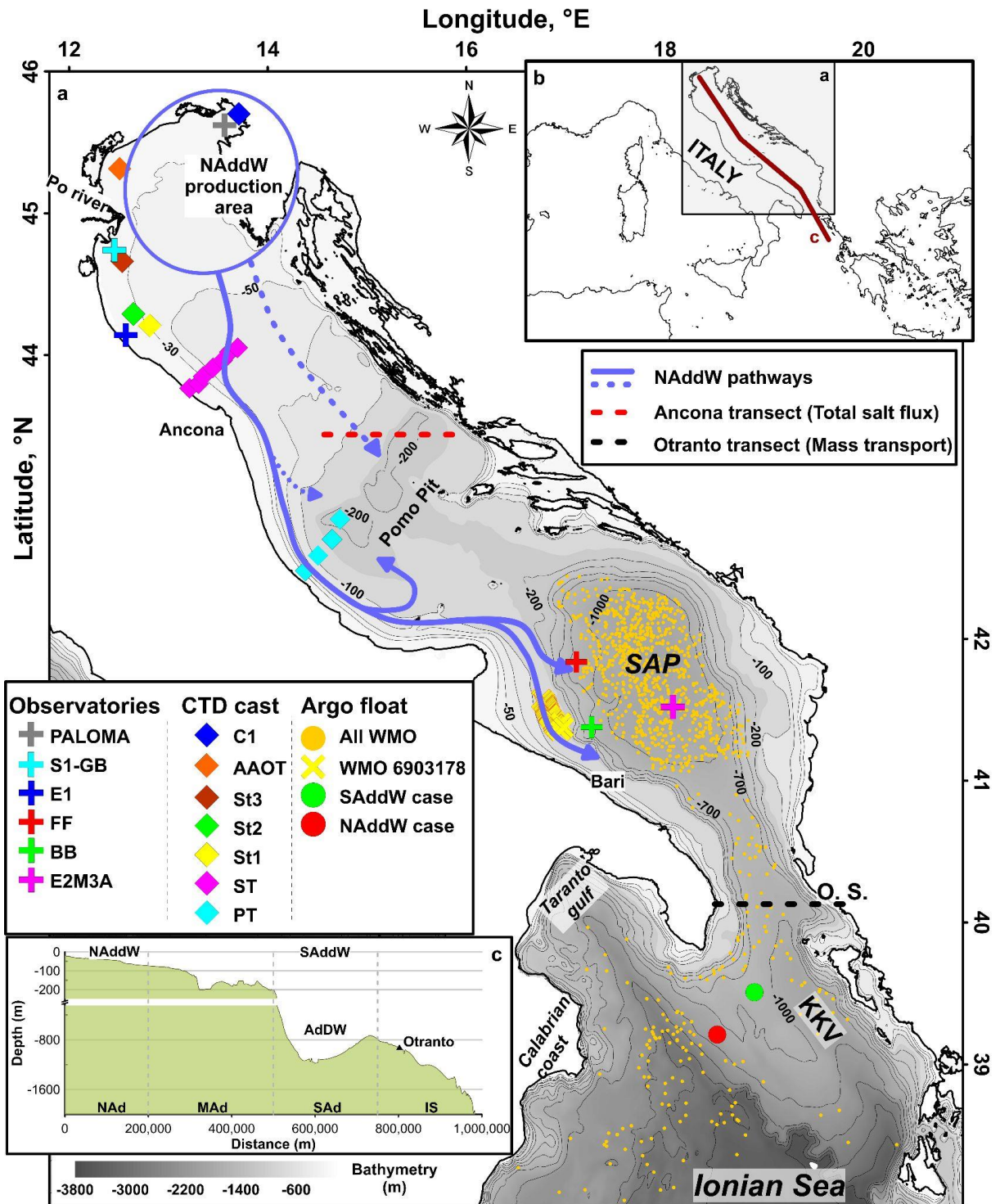


Figure 1: Main panel represents the study area with Adriatic and Ionian Sea bathymetry, pathways of the NAddW (blue line) according to Mihanovic et al., 2013; Carniel et al., 2016; Marini et al., 2016, observation network available in the study area including Argo floats, vessel surveys, moored and fixed-point observatories. The green and red circles represent the Argo data used for the Burger number calculation. The trajectory of Argo float WMO 6903178 was highlighted with a yellow cross symbol as this float was also used in figure 4 to highlight the dW passage at the edge of the SAP. Red and black dashed lines represent the sections in which the total water mass and salt transport was computed, the Ancona Section and the strait of Otranto (O.S.) respectively, using the same methods of Yari et al. (2012). KKV is Kerkira-Kephallinia Valley. In panel a regional view of the study site with the line c where the bathymetric section is extracted and represented in panel c with the main water masses in the area (NAd - Northern Adriatic, MAd - Middle

Adriatic, SAd - Southern Adriatic, IS - Ionian Sea). In panel b the Senigallia and Pomo transect are represented (ST and PT, respectively). The Bathymetry used in this figure was provided by the EMODnet Bathymetry Consortium, (doi.org/10.12770/ff3aff8a-cff1-44a3-a2c8-1910bf109f85).

2. METHODS

2.1. Dataset

Starting from the pioneering work of Zore-Armanda (1963), the knowledge of the oceanography of the Adriatic gradually grew together with the development of observation networks (Buljan & Zore-Armanda, 1966; Marini et al., 2006; Ravaoli et al., 2016; Pranic et al., 2021; Pirro et al., 2022). Data used in this study have been retrieved from different sources (Figure 1, Table S1):

- Ship surveys in the northern and middle Adriatic Sea with monthly sampling stations in the Gulf of Trieste (C1-LTER) and along the Senigallia (ST) and Pomo (PT) transects (Grilli et al., 2005; Marini et al., 2016; Cerino et al., 2019; Grilli et al., 2020; Neri et al., 2022).
- Fixed-point observatories PALOMA elastic beacon (located in the deepest area of Gulf of Trieste; Cantoni et al., 2012; Ravaoli et al., 2016), S1-GB elastic beacon (located at the Po river mouth; Ravaoli et al., 2016; Barra et al., 2020), and E1 buoy (off the coast of Rimini, Böhm et al., 2016; Ravioli et al., 2016).
- CTD profiles from “Acqua Alta” Oceanographic Tower (AAOT) located at the margin of the bora-driven northern Adriatic gyre, where the peak of dW formation is normally located (Boldrin et al., 2009).
- Vessel surveys at monitoring stations St1, St2 and St3, obtained from Sea Data Net Portal (Grilli et al., 2005).
- The moorings of South Adriatic Regional Facility of the EMSO-ERIC consortium (De Santis et al., 2022) consisting of the E2M3A “South Adriatic Pit Observatory” (Cardin et al., 2020) and Moorings BB and FF located at 600 and 733 m depth, respectively, in the main flow branch of the Bari Canyon and in the open sector of the continental slope (Turchetto et al., 2007; Langone et al., 2016; Paladini de Mendoza et al., 2022).
- Argo floats (last access available <https://dataselection.euro-argo.eu/>, last accessed on 17/07/2024. Argo (2024); Wong et al., 2020) within the SAP, in the strait of Otranto and the Ionian Sea and along the western margin of the southern Adriatic basin near the Bari Canyon where the Argo float WMO 6903178 stayed for almost a year and half.
- The Po River discharge measured at the Pontelagoscuro hydrological station (<https://www.arpae.it/it/temi-ambientali/acqua/dati-acque/acque-superficiali/dati-idrometrici-in-tempo-reale-1>).

Moreover we use high resolution observational and assimilated datasets from the Copernicus Marine Service :

1. Mediterranean Sea Physics Reanalysis (https://doi.org/10.25423/CMCC/MEDSEA_MULTIYEAR_PHY_006_004_E3R1, Escudier et al., 2020, 2021; Nigam et al., 2021).

2. High-resolution and ultra-high-resolution satellite data of the sea surface temperature of the Mediterranean Sea (<https://doi.org/10.48670/moi-00172>, Buongiorno Nardelli et al., 2013);
3. Sea Level European Seas Gridded L4 Sea Surface Heights (Rio et al., 2014) and Derived Variables Reprocessed 1993-Ongoing (<https://doi.org/10.48670/moi-00141>)-*Copernicus Climate Change Services*: ERA5 (Hersbach et al., 2020) data at individual levels from 1940 to present ([doi.org/ 10.24381/cds.adbb2d47](https://doi.org/10.24381/cds.adbb2d47)) - *Climate prediction Center (NOAA)* Northern Hemisphere large scale teleconnection patterns indexes (NAO, EA, EAWR, SCAN), (www.cpc.ncep.noaa.gov/data/teledoc/ea.shtml, last accessed 8/8/2023).

The mixed layer depth (MLD) in the SAP was calculated from the Argo data according to the method described in de Boyer Montégut et al. (2004) (i.e., using 0.2°C and 0.03 kg m^{-3} as thresholds, Kokkini et al., 2020). The σ_{θ} in all datasets is computed using thermodynamic equation of seawater - 2010 (TEOS-10, McDougall & Barker, 2011).

The net heat flux (Figure 2a) was calculated using the same method as Pirro et al. (2022) on climate data from Copernicus Climate Change Services.

Salt (TSF, Figure 2a) and mass (Figure 5d and e) transport over the sections (Ancona, 43.4°N ; $14.6-16^{\circ}\text{E}$ and Otranto, 40°N ; $18.5-19.5^{\circ}\text{E}$, Figure 1) were obtained according to the method of Yari et al. (2012), using the Mediterranean Sea Physics Reanalysis dataset. This dataset reflects well the physical dynamics of the studied area. EOF analysis, computed on Temperature and Salinity, showed strong agreement between model and observational data in the SAP, with $>90\%$ variance explained by the first modes ($R^2 > 0.9$) (Martellucci et al., 2024). The σ_{θ} values used in Figure 6b were obtained from this dataset as well.

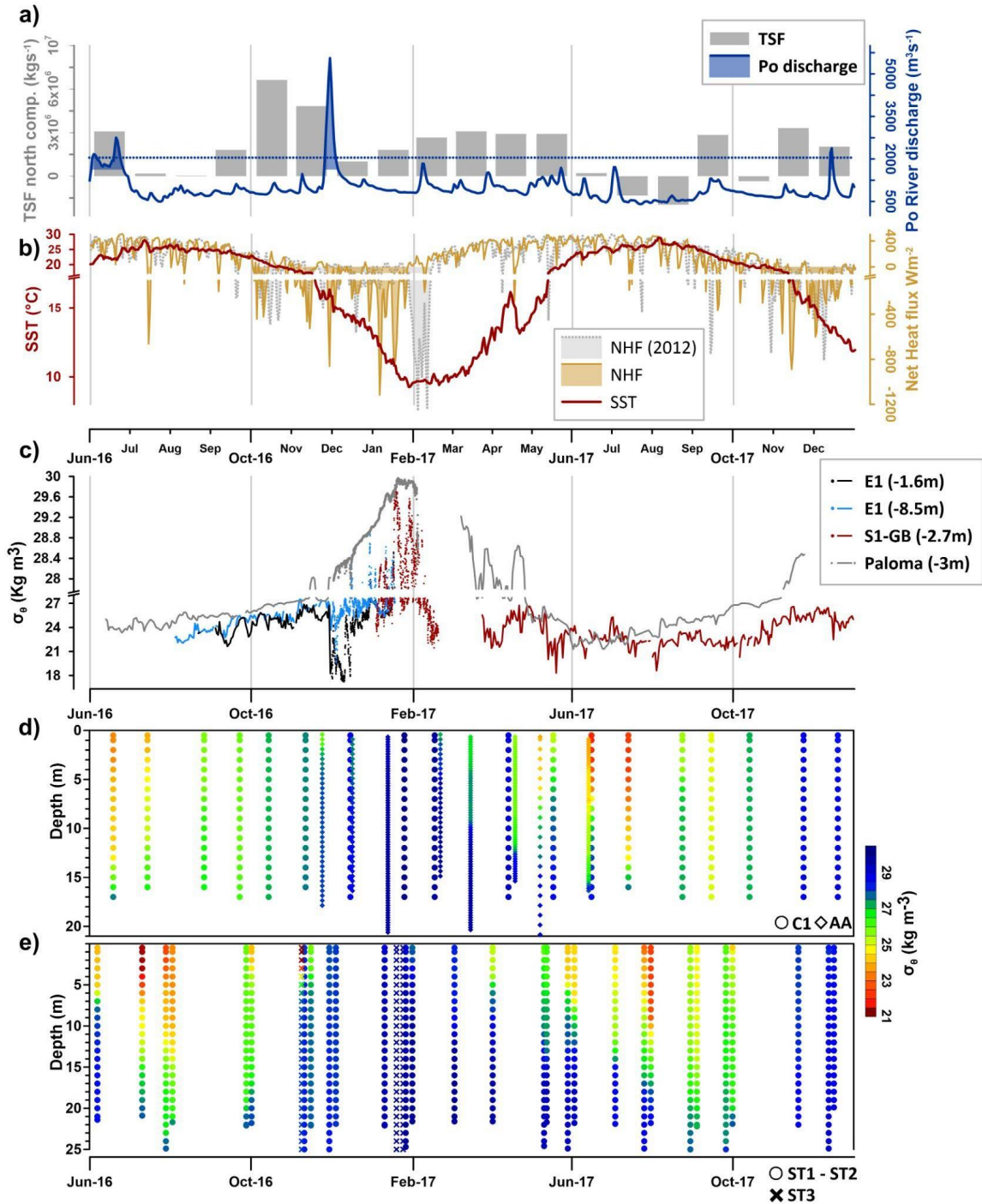
The σ_{θ} used in the Burgher number computation (Rétif et al., 2024, Tassigny et al., 2024, detailed in Section 2.3) for the South Adriatic and Ionian Sea (green triangle and square in Figure 1) were obtained from Argo float profiles during January-February 2017, considering a depth between 600 and 800 m. Conversely, for the NAddW case, σ_{θ} was considered in the 70-120 m depth layer in May 2017 in the South Adriatic shelf (Figure 2b) and in the Ionian Sea (green circle in Figure 1). The acronyms for the water mass used in this paper follow the recommendation suggested in Schroeder et al. (2024), where lowercase “d” means dense while capital “D” means deep.

2. Discussion of the observed results

2.1. Preconditioning and formation of the NAddW in the early 2017

The Po River discharges, in 2016-2017, were characterised by a peak of $5559 \text{ m}^3\text{s}^{-1}$ in late November - early December 2016 although the discharges remained consistently low throughout the autumn-winter period (below the 10-year average of the dashed blue line in Figure 2; see details in Paladini de Mendoza et al., 2023b). In the same period, an inflow of saline water from the south (Figure 2a) was observed in the northern Adriatic basin (~ 38.9 , Matic-Skoko et al., 2022) similar to what happened in 2012 (Mihanovic et al., 2013; Janekovic et al., 2014). The total salt flux (TSF, Figure 2a) calculated on the eastern side of the middle Adriatic along the Ancona transect (Figure 1) showed a peak in October-November 2016 ($\text{TSF} > 7 \times 10^6 \text{ kg s}^{-1}$), which was due to the cyclonic state of the NIG (Menna et al., 2021; Mihanović et al., 2021). The latter brought the salt waters of Levantine and

226 Aegean origin toward the northern part of the Adriatic Sea (Matić-Skoko et al., 2022) again as it was
 227 observed in 2012 (Mihanović et al., 2013; Janeković et al., 2014).
 228



229
 230 Figure 2: a) Time series of the Po River discharge measured at Pontelagoscuro (blue line). The line is filled in blue if the
 231 discharge is greater than the average 10-year discharge value. Total salt flux, TSF (grey boxes) computed from CMS
 232 Physical Reanalysis (Escudier et al., 2021) dataset according to the method of Yari et al. (2012). b) Sea Surface
 233 Temperature, (SST, dark red line) and Net Heat Fluxes (NHF) averaged over the northern Adriatic area for 2017 (golden
 234 shaded filled line) and 2012 (dotted grey filled line, same period of 2017, the time axis for the year 2012 is not shown)
 235 Data from Mediterranean Sea Physics Reanalysis. c) Hourly σ_θ values calculated from the CTD records available for the

studied period at the PALOMA elastic beacon, at the E1 buoy and at the S1-GB elastic beacon, at two depths d-e) Time series of σ_θ in the northern Adriatic shelf area (see Figure 1). Panel d represents the σ_θ profile sampled at C1-LTER (circle) and Acqua Alta (AA, diamond), while in panel e the circles represent St1, the squares St2, and the crosses represent the northernmost station St3.

Synoptic atmospheric configuration in January 2017 drove significant strong heat losses over the northern Adriatic region. Between December 29, 2016 and January 18, 2017, a strong cold air outbreak occurred (Figure 2b), comparable to the event in February 2012 shown by the filled dotted line in Figure 2b ($>1100 \text{ Wm}^{-2}$, peaking at 1250 Wm^{-2} on February 4, 2017). The associated sea surface temperature drop was about 8°C (Figure 2b).

The strong heat losses recorded over the area took place in presence of a negative state of the East Atlantic (EA) pattern (-1.15), the second prominent mode of atmospheric variability in the North Atlantic. This general circulation pattern is widely recognized as an important driver of heat losses in the Mediterranean region (Josey et al., 2011; Reale et al., 2020). Its negative state is associated with a significant northeasterly air flow driven by an area of high pressure over the western Atlantic bringing cold and dry air from mainland Europe into the Mediterranean region (Josey et al., 2011), driving strong heat losses (Figure 2b). Negative states in the EA were observed as well in January and February 2012 (-1.76 and -1.73 respectively).

The combination of heat losses, low discharge in the autumn and advection of saltwater (Figures 2a, 2b) was the precondition for the formation of very dense NAddW with signature of densification that was clearly visible at the elastic beacon PALOMA and at the C1-LTER station in the Gulf of Trieste, in early December (Figure 2c,d), peaking ($\sigma_\theta = 29.94 \text{ kg m}^{-3}$) on January 20 after the strong heat loss and remained high ($\sigma_\theta > 29.8 \text{ kg m}^{-3}$) until the first week of February (Figure 2c). The same temporal trend was also observed in the profile of the Acqua Alta station where the σ_θ reached 29.55 kg m^{-3} on January 12 (Figure 2d).

After its formation, the NAddW flowed along the Italian coast, generating maxima of σ_θ of 29.70 kg m^{-3} at buoy E1 and S1-GB elastic beacon on January 18, 2017 (Figure 2c). Similarly, on St1 and St3 the density increased throughout the water column from late December to the end of January, reaching 29.4 kg m^{-3} . The increase in seawater density above 29.6 kg m^{-3} in the surface layer lasted for almost 2 days (January 17-20), involving the whole water column (i.e., density profile in St1, St2 and St3) and capturing the dW flow. Then, from the end of January, the surface density decreased to the values observed prior to December while the signature of dW below 15 meters depth remained evident until April (Figure 2d). In late spring, the near-bottom dW on the shelf (Figure 2c) was replaced by lighter ($<27 \text{ kg m}^{-3}$) adjacent water as observed in previous dW events (Orlić et al., 2006; Vilibić et al., 2023).

After its formation in the northern Adriatic, the first signature of the NAddW was detected 100 km to south of St1 in the Pomo Pit in February 2017 (Neri et al., 2023). The comparison of repeated CTD profiles from June 2016 to May 2017 along the Senigallia and Pomo transects (ST, PT), (Figure 3), show the change in the thermohaline properties of the water masses. By December 2016, the water column had changed from stratified to well-mixed, with the σ_θ increasing from 28.6 kg m^{-3} to over 29.6 kg m^{-3} on February 11 (Figure 3a). The dissolved oxygen (DO) concentration (Figure 3b) shows a strong increase of about $30 \mu\text{mol L}^{-1}$ from December to February in all transects, up to $260 \mu\text{mol L}^{-1}$. In May, the σ_θ decreased while the DO concentration reached its maximum between 20 m

and 55 m (between 274 and 305 $\mu\text{mol L}^{-1}$), suggesting a strong contribution of biological production (Neri et al., 2023). The dW signal (Figure 3a, b) was clearly observed in the Pomo Pit (i.e., σ_θ in the farthest offshore station of PT section), presenting the same values observed in February along the ST transect (Figure 3a) spanning almost 30 km in the cross section. The dW were found in the deepest layer of the Pit (> 160m depth, i.e., σ_θ reaches 29.6 kg m^{-3} in the terminal part of the profile), highlighted by the maximum in σ_θ as except for the shallowest station, that was not affected by dW passage.

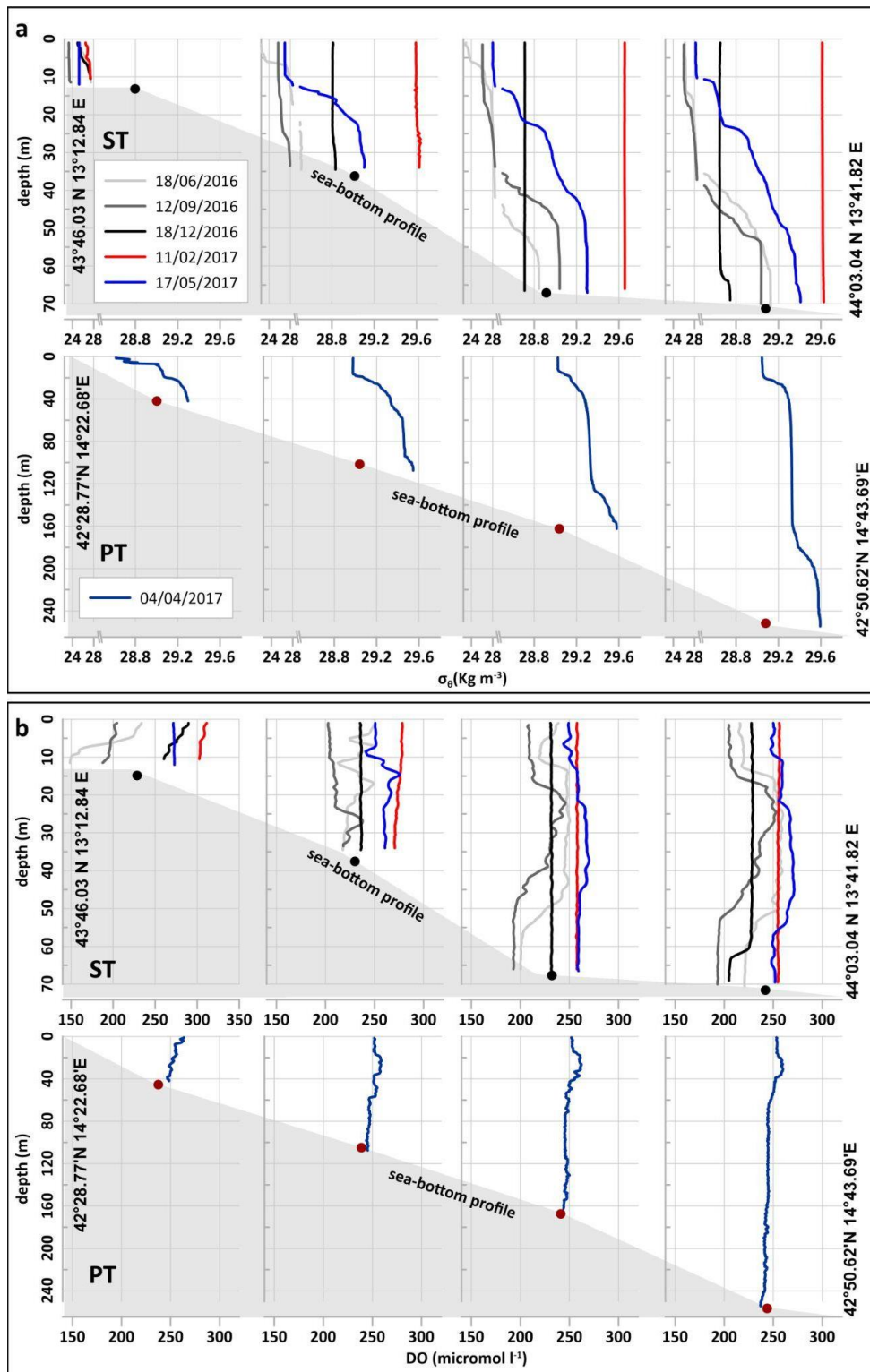


Figure 3. Shipboard CTD profiles (σ_θ and DO), repeated from June 2016 to May 2017 along the transect of Pomo (PT) and Senigallia (ST) (see Figure 1b for the transects location).

2.2 Spreading of NAddW in the southern Adriatic

The timing of the occurrence of the NAddW in the southern Adriatic depends on its travel dispersal through the Pomo Pit (Janeković et al., 2014; Benetazzo et al., 2014), which is driven by the density

gradient between the NAddW and the adjacent waters (Vilibić & Mihanović, 2013; Querin et al., 2016). The timing of the arrival of NAddW to the continental margin of the southern Adriatic after its formation is not yet clearly defined but considering previous studies we can consider a rough median value of about two months (Bensi et al., 2013; Querin et al., 2016; Chiggiato et al., 2016; Vilibić et al., 2023, Le Meur et al., 2024) and lasts about six months. The observations (Figure 4a and c) of the Argo float WMO 6903178 at the shelf edge of the Bari Canyon (June 2016 - December 2017) show a well-stratified water column until January 2017, when the σ_θ ranged from 25.5 kg m⁻³ in the surface layer (supersaturated colour in Figure 4a) to 29 kg m⁻³ near the bottom. The stratification, clearly visible until September 2016, was influenced by the Western Adriatic Current (WAC), which is characterised by low salinity (Mauri et al., 2016). A high DO concentration was observed in the water column (between 20 m and 60 m) until November 2016 (>240 µmol L⁻¹), while below 60 m the concentration gradually decreased from June 2016 until the onset of winter mixing at the end of December (Figure 4c), when it increased again to 226-232 µmol L⁻¹. From June 2016 to January 2017, a stable increase in the σ_θ signal (Figure 4b) is observed when moving from the shelf edge towards the great depths of the SAP at 1200 m (average value of 29.15 kg m⁻³, between June 2016 and May 2017). In fact, until January 2017 the σ_θ in BB in the Bari Canyon at 590 m depth fluctuated around the mean value of 29.12 kg m⁻³, while it was more stable and slightly higher (29.17 kg m⁻³) in the deeper areas of the open slope (in FF). The measurements of the Argo floats during the same period in the SAP (within the 1000 m isobath) show homogeneous thermohaline properties corresponding to the fixed observations of E2M3A .

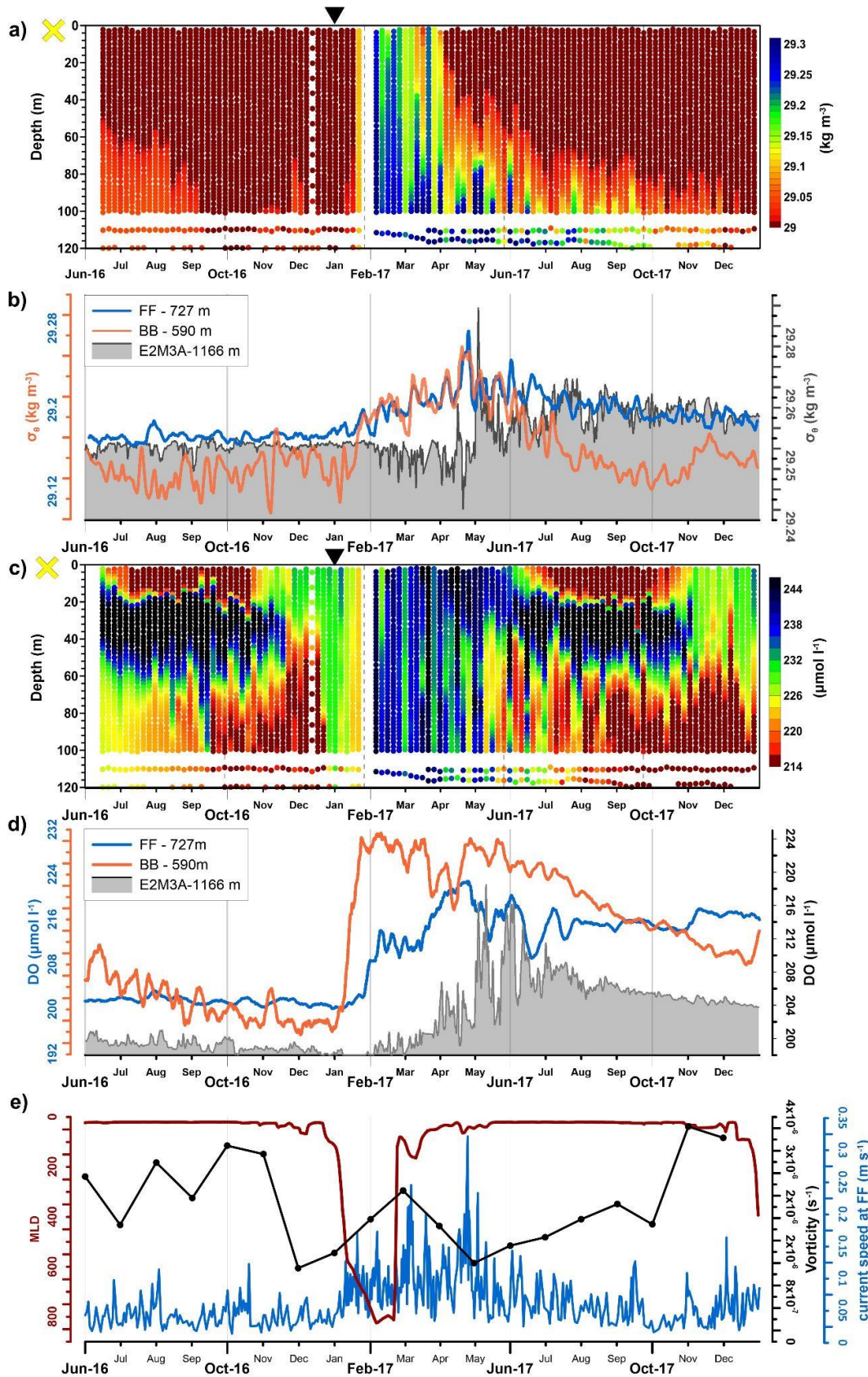


Figure 4: Density and DO Argo float WMO 6903178 observations in the shelf area near the Bari Canyon (a, c; yellow cross in Figure 1) and at BB, FF and E2M3A (b, d; yellow square, star and triangle in Figure 1). The black triangles on top of figure a and c indicate the period in which the float sampled on the continental shelf (120 m depth, yellow cross in

Figure 1). (e) Vorticity field computed in the southern Adriatic Sea (black line, within the 1000 m isobath, see Menna et al., 2021) and Mixed Layer Depth (MDL, purple line) in the SAP.

In winter, the SAP, which is a site of dense-water formation (Pirro et al., 2022), was also affected by cold meteorological events with the formation of convective phenomena that mixed the water column down to 800 m depth (Figure 4e) altering its thermohaline properties (Kokkini et al., 2020; Mihanovic et al., 2021; Martellucci et al., 2024). The process started in January 2017 and produced the Southern Adriatic Dense Water (SAddW, Mantziafou & Lascaratos, 2004).

The deepening of the MLD to 800 m (Figure 4e) led to an increase in DO, σ_θ and current velocity, which were first detected by the shallower mooring in the Bari Canyon (BB) starting from mid-January, and after two weeks, also by the deeper northern mooring (FF) (Figure 4b, d). After the initial strong increase in DO concentration, the signal showed a gradual decline until early March.

During 2017, the strong current pulses attributed to the cascading NAddW flow were clearly detected from early March (particularly evident at the FF site), when a renewed increase in σ_θ and DO concentration occurred due to the arrival of NAddW cascading down the slope. The current velocity behaviour (Figure 4e) recorded at the open-slope (FF) shows the passage of NAddW as intermittent strong pulses (Marini et al., 2016; Chiggiato et al., 2016; Paladini de Mendoza et al., 2023a) as a result of the propagation of the continental shelf wave along the Adriatic basin (Bonaldo et al., 2016) with velocity peaks corresponding to the σ_θ and DO concentration maxima.

On the shelf, the dW current first affected the deeper layers (March 15) around 80 m depth and then (March 25) almost the entire water column ($\sigma_\theta > 29.25 \text{ kg m}^{-3}$ in Figure 4a). The same trend was also observed in the canyons, with σ_θ increases by 0.05 kg m^{-3} in BB and 0.03 kg m^{-3} in FF (Figure 4b), as well as DO content (Figure 4d). The highest σ_θ value ($> 29.4 \text{ kg m}^{-3}$) due to NAddW was observed at the end of April, with a duration of 5 days, resulting in the highest increase in σ_θ in the canyons (BB and FF in Figure 4b). After 20 days of passage along the shelf, NAddW reached the deepest layer of the SAP (E2M3A in Figure 4b and d) and resulted in an increase in σ_θ of 0.03 kg m^{-3} at 1200 m depth and a significant increase in DO concentration (about $25 \mu\text{mol L}^{-1}$).

On the continental shelf (Figure 4a, c), the NAddW was gradually replaced by lighter water and returned to the state observed in summer and fall 2016. The passage of NAddW currents confined to the deepest layers of the water column (40 m thick) continued until September, but with a strong decrease in σ_θ , as previously observed for 2012 (Vilibić & Mihanović, 2013; Mihanović et al., 2013). These pulsations confirmed that the outflow of NAddW persisted for months after its formation (Figures 2c, 4a and 4b).

The downward motion of NAddW contributes to the filling of the deeper layers of the Adriatic (Figure 4a) resulting in an increase of the temperature of 0.1°C and salinity of 0.05, which affected the wider Adriatic circulation.

At the beginning of the winter, a decrease in the vorticity field in the SAP (Figure 4 e) was observed, which reached its minimum in May 2017, coinciding with the maximum increase in the σ_θ at BB and FF. The observations indicate that the changes in the vorticity field observed in winter and spring were caused by the combined effect of convection on the open ocean and NAddW propagation, which influence the hydrodynamic, thermohaline and biochemical properties of the SAP. The effect of convection causes a homogenization in the SAP, which leads to a change in the isopycnals and

consequently in the density gradient within the SAP. At the same time, the presence of dW at the western edge of the Adriatic in turn causes a decrease in the density gradient of the baroclinic component of the cyclonic vorticity field.

2.3 Spreading in the Ionian Sea

Until February 2017, the thermohaline properties of the strait of Otranto remained almost stable, while after February a general increase in density, temperature and salinity was observed (Figure 5a, b).

The transport in the deep layer below 400 m across the section in the strait of Otranto (Figure 5a), was southwards and exhibited strong variability. The largest amount of outflow occurred during the convection period (February - March), which is related to the open-ocean convection in the SAP and the formation of SAddW (i.e. deepening of the MLD in Figure 4e). After the convection period the outflow was related with the outflow of NAddW and AdDW (Manca et al., 2002) identified by marked decreases in temperature and salinity (Figure 5a) occurring in April and July. These three different water masses have been generated by the three temperature and salinity changes (Figure 5b), which also correspond to the peaks observed at the moorings (BB, FF and E2M3A), although shifted in time.

The signature of this peak appears in the TS diagram of Figure 5d, which highlights an overall increase in the density field of about 0.02 kg m^{-3} above the isopycnal value of 29.2 kg m^{-3} .

Crossing the strait of Otranto the overflow water mixed during transport, highlighted by a decrease in the σ_θ ($\sim 0.02 \text{ kg m}^{-3}$). σ_θ values in the Ionian Sea are consistent with the measurements of Kovačević et al., (2015) in 2012, where the σ_θ was above 29.2 kg m^{-3} (with a maximum value of 29.26 kg m^{-3}).

Figure 5e shows the location of measurements where the density exceeds the 29.2 kg m^{-3} threshold and highlights the newly formed dW outflow from the southern Adriatic Sea into the Ionian Sea.

In June, two different water masses were observed in the northern Ionian Sea: one in the Gulf of Taranto and the other south of the strait of Otranto. The first was characterised by a temperature and salinity of about 13.8°C and 38.8 , while the second was colder with a temperature of 13.7°C and a salinity of 38.75 . Considering the area where these water masses were located and the distance from the source (i.e., SAP), they might represent the signature of the AdDW and NAddW, respectively. Data show the densest values about 50 km south of the strait of Otranto at 870 m depth on June 17 (Figure 5e). This signal is further evidence that the part of the NAddW that does not cascade down the slope towards the SAP sinks diffusely along the western continental shelf and in our case can be observed about 800 m south of the strait of Otranto after one month. This confirms and corroborates earlier results obtained in the winters of 1997/98 by Manca et al. (2002), the modelling results of Rubino et al. (2012) and the interpretation of large-scale bedform patterns by Rovere et al. (2019) and Ceramicola et al., (2024).

Compared to the earlier observations that show a branch of dW flowing along the western margin of the Ionian Sea (Sellschopp & Álvarez, 2003), our data show a double route outside the strait of Otranto. One branch of the dW current flows in the Gulf of Taranto and appears along the eastern Calabrian coast between October and December while the second branch flows down the Western Hellenic continental slope towards the Kerkira-Kephallinia Valley.

The Burger number (B_u) defined as the ratio between the Rossby radius of deformation (LR) and the horizontal characteristic length scale (L) of the strait of Otranto plays a key role in understanding the dynamics of these two distinct paths. Specifically:

$$B_u = \left(\frac{LR}{L}\right)^2$$

where $LR = \frac{\sqrt{g'H}}{f}$, with f the value of the Coriolis parameter ($9.37\text{e}^{-5} \text{ s}^{-1}$ for a mean latitude of 40° N), $H=900 \text{ m}$ and $L=80 \text{ km}$ the characteristic depth and length scale at the strait of Otranto, respectively, and $g' = \frac{g\Delta\rho}{\rho_0} = g \frac{\rho_{adriatic} - \rho_{ionian}}{\rho_{ionian}}$ the reduced gravity. A small B_u value indicates that the transport of the dW is constrained by the Coriolis effect flowing therefore, through the Gulf of Taranto. Conversely, for a large B_u value, the dW is less affected by rotation and potentially aligns with density-driven currents.

Considering the dW forming within the SAP, $\rho_{adriatic} = 1029.19 \text{ kg m}^{-3}$, computed from Argo floats profiles averaged during January-February 2017 and between 600 and 800 m of depth while, $\rho_{ionian} = 1029.16 \text{ kg m}^{-3}$ and computed for the same period in the range 600 - 800 m of depth from the Argo float highlighted by the green circle in Figure 1. This yields to $B_u (= 0.16) < 1$ explaining why the dW is deflected towards the Gulf of Taranto. Conversely, for the NAddW case, $\rho_{adriatic} = 1029.26 \text{ kg m}^{-3}$, calculated in the SAP for the layer 70-120 m of depth and for May 2017 (red circle in Figure 1) while, $\rho_{ionian} = 1029.015 \text{ kg m}^{-3}$, computed for the same period and depth range from the Argo float shown by the green triangle in Figure 1. This yields to $B_u (= 1.33) > 1$ allowing the dW to flow southwards resulted in a strong release of the densest NAddW through several passages along the Northern and Western perimeter of the SAP causing an important weakening of the Southern Adriatic Gyre (Figure 4e).

The dW outflowing from the strait of Otranto resulted in a strong release of dW in the Ionian Sea causing important variation in the vorticity field of the NIG (Figure 6), which is related to the change in density gradient in the Ionian basin. As Rubino et al. (2020) and Gačić et al. (2021) have already shown, the outflow of dW leads to a reversal of the circulation in the Ionian Basin, making it anticyclonic and favouring the presence of water of Atlantic origin in the northern part of the Ionian Sea.

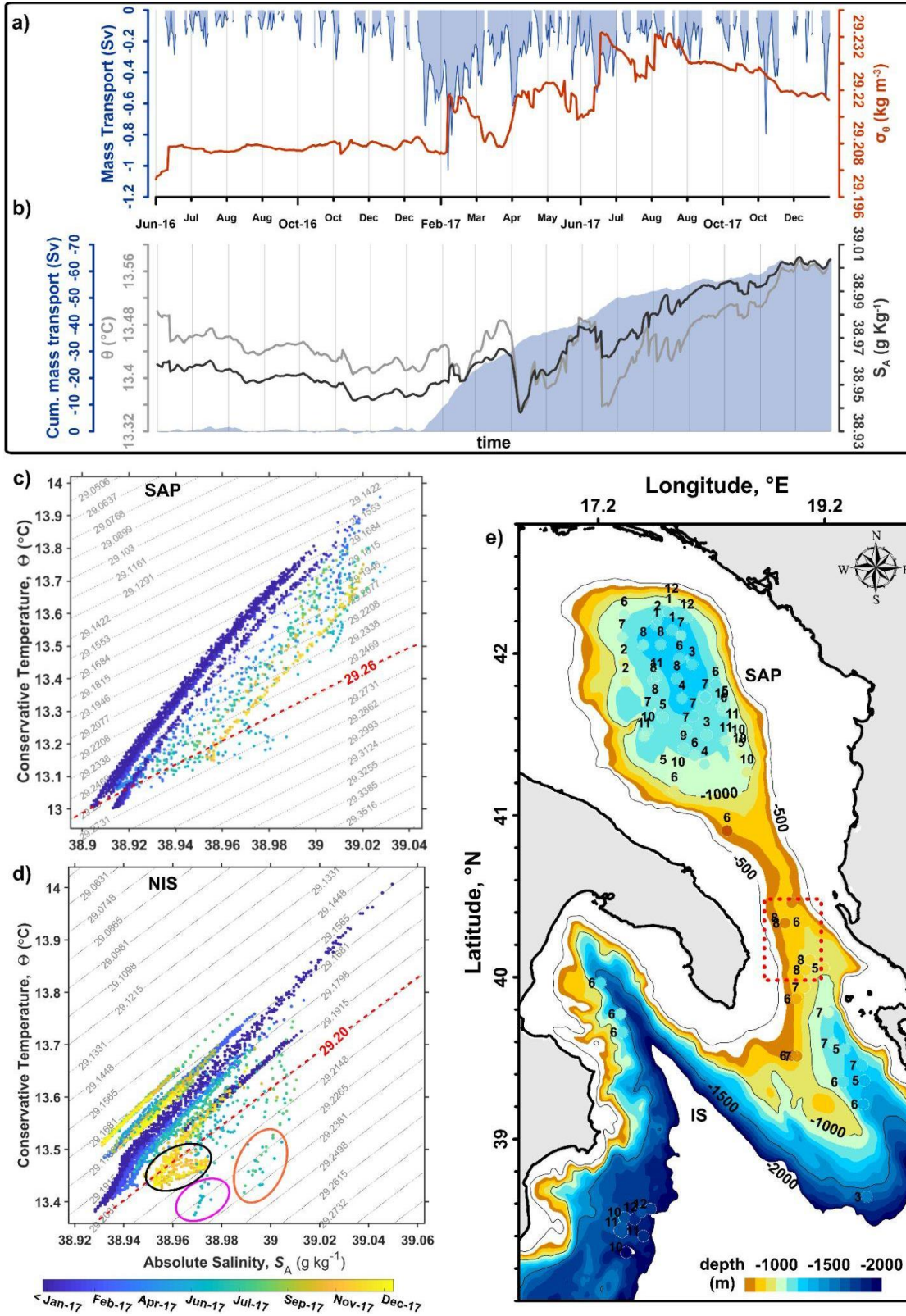


Figure 5. Top panel; a) Time-series of mean σ_θ (red line), calculated in the red dashed box in the map e, and water mass transport (blue filled area) across the Otranto section between 400 m and bottom (O.S., dashed black line in Figure 1); b) time-series of mean temperature (grey line), salinity (black line) calculated in the red dashed box in the map e and cumulated mass transport (blue filled area), across the Otranto section between 400 m and bottom. Bottom panel: TS diagrams of the Argo measurements in the SAP (c) and in the northern Ionian Sea (d) below 800m. The coloured circles

in panel d indicate the different water masses orange: AdDW, magenta: NAddW, black: SAddW; e) Map with the positions of the measurements that exceeded the density 29.2 kg m^{-3} threshold (red dashed lines in a and b, numbers refer to the corresponding months of each observation).

The change in circulation is clearly visible in Figure 6a. During winter 2017, the minimum height and cyclonic circulation with northward current along the east coast of the basin favoured the flow of Levantine waters near the strait of Otranto, and a broad current from the Sicilian Channel flowing eastward toward the Levantine basin. Between May and June, a decrease in the Levantine flow northward is observed, and between July and August the circulation becomes anticyclonic. From November, a new decrease in the anticyclonic phase is observed, brought about by an area of low pressure in the eastern part of the basin and the interruption of Atlantic water flow from the Sicilian Channel. These changes also affect the vertical dynamics of the water column, which results in a change in the arrangement of isopycnals (density sections of Figure 6b in the two phases of February and October).

In February, when the cyclonic circulation prevails, the vertical circulation is characterized by upwelling in the central part, with higher surface salinity. In October, during the anticyclonic phase, downwelling is observed in the centre of the basin, which is reflected in the general decrease of salinity in the northern Ionian Sea, as can be seen from the strong density change in Figure 6b. The results suggest an impact of dW dynamics on the reversal of the northern Ionian Gyre adding new findings to recent work that investigated the causes of this rotation using both laboratory experiments and model simulations (Gačić et al., 2010; Reale et al., 2017; Reale et al., 2016; Rubino et al., 2020; Gačić et al., 2021; Liu et al., 2022; Eusebi-Borzelli & Carniel, 2023; Eusebi-Borzelli et al., 2024; Mieli, 2024). The sinking into the Kerkyra-Kefalonia Valley and consequent spreading into the Hellenic Trench by a fairly dense and fast flow does not feed the flow toward the gulf of Taranto responsible for the reduction of the vorticity field in the northern Ionian Sea with a limited impact on the NIG rotation.

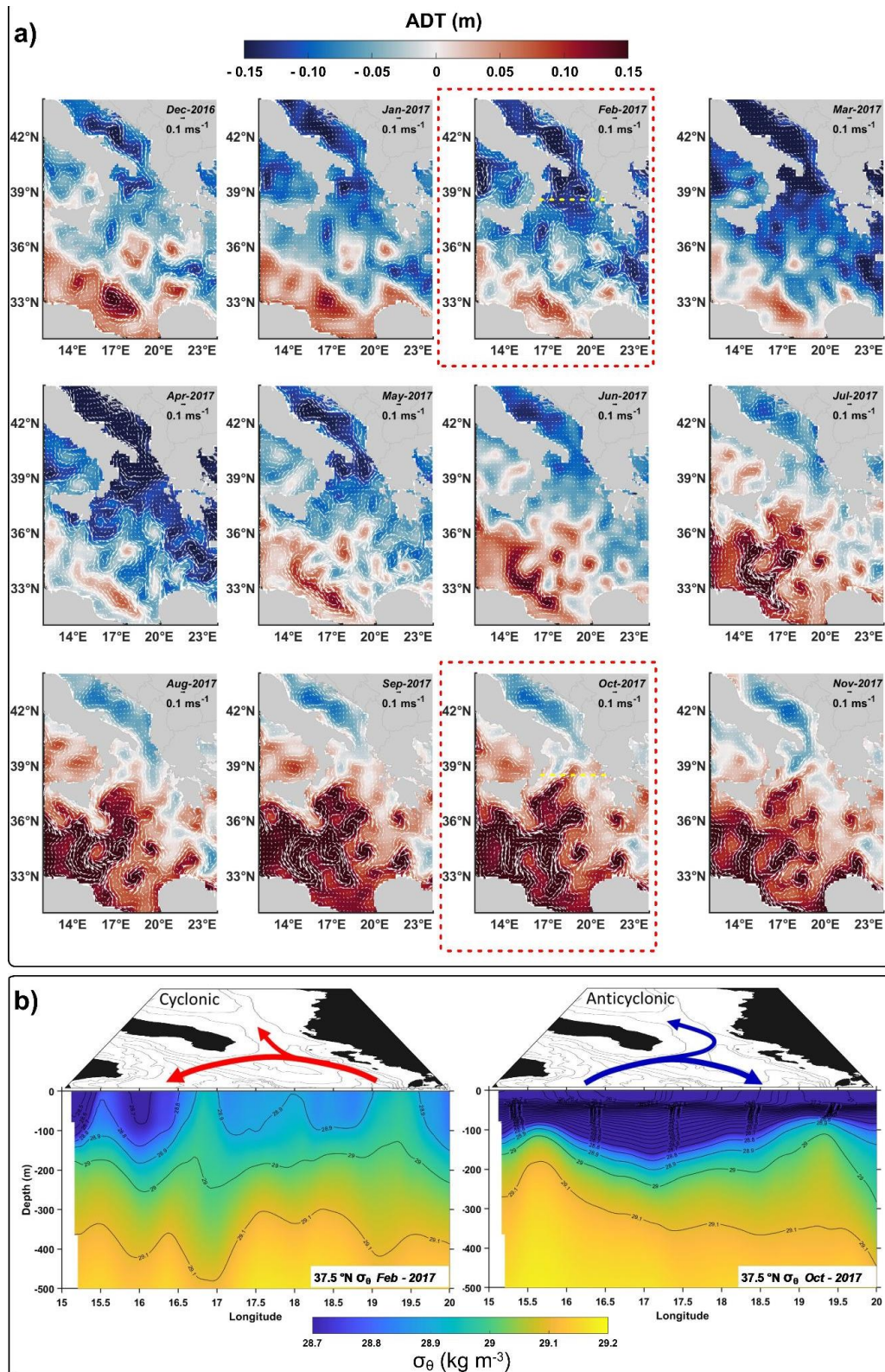


Figure 6. a) Monthly mean geostrophic currents (arrows) superimposed on monthly mean distribution of ADT (colours) for the period June 2016–December 2017 (<https://doi.org/10.48670/moi-00141>); b) Water column distribution of the σ_θ (computed from MEDSEA_MULTIYEAR_PHY_006_004_E3R1) along a transect crossing the Ionian Sea at 37.5°N (yellow dotted lines of panel a). during the two different circulation phases (cyclonic and anticyclonic, months enclosed in red boxes of panel a).

3. Summary and Conclusion

The Mediterranean Sea is a complex and interconnected system where the deep water circulation plays a key role in the local ecosystem dynamics. The national observatory network built in the Adriatic Sea, (including coastal fixed stations, deep moorings , Argo floats and vessel surveys) represents a unique sea laboratory where complex ocean processes can be studied. In this study, the observational and modelling systems available for the area enabled us to follow the route of dW from its source revealing new dynamics and implications of ocean circulation at basin scale and in the Eastern Mediterranean circulation system.

The autumn-winter period 2016-2017 was characterised by conditions that favour enhanced dW formation (Figure 2a): low Po River discharge, inflow of Levantine salty water from the south (Matic-Skoko et al., 2022) driven by the five years of cyclonic phase of the NIG (Menna et al., 2022), and strong heat losses in the northern Adriatic region (Josey et al., 2011; Reale et al., 2020) triggering the formation of the NAddW as well as the SAddW (Table 1).

After its formation, the dW mass flows southward following the Italian coast and its thermohaline characteristics change sensitively along the route with the range of variation strictly dependent on the variability of the drivers (Sellschopp & Alvarez, 2003). The comparison between the 2017 dW formation ($\sigma_\theta = 29.94 \text{ kg m}^{-3}$ at PALOMA and 29.55 kg m^{-3} at AAOT, Figure 2 c, d) and that of 2012, the coldest ever recorded (Bensi et al., 2013; Mihanović et al., 2013; Raicich et al., 2013; Vilibić et al., 2023), reveals that denser waters were produced in 2012 (30.59 kg m^{-3} and 30.35 kg m^{-3} in the Gulf of Trieste and at the AAOT station, Mihanovic et al., 2013). Considering that the 2017 heat loss was comparable with that of 2012 in terms of absolute values, the main difference in NAddW densification can be related to: a) the exceptionally long duration of the 2012 cold break event, (it lasted almost two weeks), b) the timing (in 2017 the strong heat loss occurred in early January) and c) the general 2017 positive trend in temperature that involved both the Adriatic Sea (Mihanović et al., 2021; Menna et al., 2021, 2022) and the Mediterranean basin (Pastor et al., 2020; Fedele et al., 2022; Kubin et al., 2023). The density difference between the two years is also evident in the Pomo Pit: in 2012, the NAddW was characterised by σ_θ in the range of 29.67 kg m^{-3} and 29.69 kg m^{-3} while in 2017 the observed value was around 29.60 kg m^{-3} .

The passage of the NAddW along the continental margin of the southern Adriatic has been clearly detected since early March 2017 (Figure 4) through the physical and biochemical changes in seawater properties in phase with strong intermittent current pulses (i.e., velocity peaks corresponding to σ_θ and DO concentration maxima in Figure 4). During January 2017, coinciding with the formation of NAddW, open-ocean convection in the SAP (Mihanović et al., 2021) mixed the water column down to 800 m depth (Figure 4e) forming the SAddW, which is the first source of dW spreading into the Ionian Basin. This water mass, once-formed, outflows from the strait of Otranto until early March 2017 (Figure 5a) with a peak in early February 2017 (0.7 Sv). After about 20 days from the cascading event into the Bari Canyon, the NAddW reached the bottom of the SAP of the SAP causing a decrease in vorticity associated with an increase in horizontal current velocity observed at the two mooring sites (Figure 4b c). At the end of May 2017, simultaneous measurements of the E2M3A site and the Argo float in the SAP showed changes in the thermohaline

properties, which can be attributed to the formation of AdDW resulted from the mixing of the deep water of the SAP with the NAddW (Manca et al, 2002; Querin et al. 2016; Vilibić et al., 2023).

The dW, which originates in the Adriatic Sea, spreads at different times in the Ionian Basin where three different water masses were recognised (Figure 5d): the newly formed SAddW after the convection event, the NAddW water mass and the AdDW formed from the mixing of resident water from the southern Adriatic and NAddW. As also observed by Gačić et al. (2014) in 2012 the σ_θ of these dW ranged from 29.2 to 29.3 kg m⁻³ in the deep Ionian Sea. The densest values were measured outside the strait of Otranto since late June. This provides evidence that the part of the NAddW not cascading down the slope towards the SAP sinks diffusely along the western continental shelf, flowing via a double route into the Ionian Sea. One branch of the dW current runs westwards towards the Gulf of Taranto (Bignami et al., 1990; Manca et al., 2002; Ursella et al., 2012; Gačić et al., 2014; Kovacevic et al., 2015; Rovere et al., 2019) while a second branch breaks the geostrophic constraints down the Western Hellenic continental slope directing towards the Kerkira-Kephallinia Valley down the Western Hellenic continental slope at depth greater than 3000m. The westward dW flow to the Gulf of Taranto favours the reversal of the NIG, and changes the isopycnal displacement in the Ionian Sea (Figure 6b). In a cyclonic eddy structure, a dense flow at the edge leads to a reduction or inversion of the vorticity field (Gačić et al., 2021). Consequently, we can assume that a very dense and rapid outflow from the strait of Otranto sinking directly southward into the Kerkira-Kephallinia Valley and spreading directly into the Hellenic Trench does not reverse the surface circulation of the NIG.

To explain this we can focus on the 2012 cold outbreak, when the densest NAddW formed, and the vorticity field in the northern Ionian Sea was anticyclonic for only six month (Gacic et al 2014, Kovacevic et al., 2014, Menna et al., 2022), appearing marginally influenced by dense water cascading (Borzelli et al., 2023 and 2024).

The largest amount of dW cascaded directly into the Kerkira-Kephallinia Valley and reached the Hellenic trench in a few months, thus mainly affecting the Levantine basin, while only a small part of dW, produced during the most intense dW formation event ever recorded, followed the western route, contributing to the NIG inversion.

Within the context of an evolving global climate, the dW formation events in 2017 represent a profound manifestation of the intricate interplay between the atmosphere and ocean. The rise in ocean temperature observed in recent years in the Mediterranean Sea could favour the production of (Pastor et al., 2020) warmer NAddW unable to reach the deepest part of the Eastern Mediterranean Sea with direct consequence on deep heat transfer and ventilation. The density values of 2017 reflect the combined effects of temperature and salinity balance, making NAddW dense enough to spread in the deep layers of the Eastern Mediterranean basin. However considering the current case of the North Western Mediterranean Sea (i.e., 10 years without strong dW events, Josey & Schroeder, 2023; Li et al., 2024) and the climate projection (Darmaraki et al., 2019; Parras-Berrocal et al., 2022 and 2023; Reale et al., 2022), salinification may not fully counterbalance the increase in temperature. As a result, the NAddW could become less dense and fail to reach the deepest layers of the Eastern Mediterranean, potentially causing significant impacts on deep ocean ecosystems.

Data Availability Statement

The bathymetry data were obtained from EMODnet Bathymetry Consortium, (doi.org/10.12770/ff3aff8a-cff1-44a3-a2c8-1910bf109f85).

Physical and biogeochemical measurements were obtained from the different network platforms (see table S1).

Climate index were obtained from *Climate prediction Center (NOAA)* Northern Hemisphere large scale teleconnection patterns indexes (NAO, EA, EAWR, SCAN), (www.cpc.ncep.noaa.gov/data/teledoc/ea.shtml, last accessed 8/8/2023).

Atmospheric forcing data were obtained from the European

Centre for Medium-Range Weather Forecasts at <https://climate.copernicus.eu/climate-reanalysis>.

The Po River discharge data were obtained from the at the website <https://www.arpae.it/it/temi-ambientali/acqua/dati-acque/acque-superficiali/dati-idrometrici-in-tempo-reale-1>.

High resolution observational and assimilated datasets were obtained from Copernicus Marine Environment Monitoring Service at <http://marine.copernicus.eu/>.

Acknowledgments/Founding

We thank the National Recovery and Resilience Plan of Italian Ministry of University and Research funded by EU – Next Generation EU Mission 4 “Education and Research” – Component 2: “From research to business” – Investment 3.1: “Fund for the realisation of an integrated system of research and innovation infrastructures” – Project IR0000032 – ITINERIS – Italian Integrated Environmental Research Infrastructures System – CUP B53C22002150006. The authors acknowledge the Research Infrastructures participating in the ITINERIS project with their Italian nodes: ACTRIS, ANAEE, ATLaS, CeTRA, DANUBIUS, DISSCO, e-LTER, ECORD, EMPHASIS, EMSO ,EUFAR ,Euro-Argo, EuroFleets, Geoscience, IBISBA, ICOS, JERICO, LIFEWATCH, LNS, N/R Laura Bassi, SIOS, SMINO.

This research was also funded by the Italian Ministry of University and Research as part of the ARGO-ITALY program. Argo float data and metadata from Global Data Assembly Centre (Argo GDAC), SEANOE, <https://doi.org/10.17882/42182>, 2024.

“Acqua Alta” Oceanographic tower (the measuring observatory of the Gulf of Venice research site; <https://deims.org/758087d7-231f-4f07-bd7e-6922e0c283fd>), the fixed-point observatories E1 and S1-GB (part of the “Delta del Po and Costa Romagnola” research site; <https://deims.org/6869436a-80f4-4c6d-954b-a730b348d7ce>) and the Senigallia Transect (ST; <https://deims.org/be8971c2-c708-4d6e-a4c7-f49fcf1623c1>) belong to the Long Term Ecological Research national and international networks (LTER-Italy, LTER-Europe and ILTER) and to eLTER Research Infrastructure. Acqua Alta Oceanographic tower and the S1-GB elastic beacon are also part of the Danubius and JERICO Research Infrastructures.

St1 St2 and St3 data were provided through SeaDataNet Pan-European infrastructure for ocean and marine data management (<https://www.seadatanet.org>).

EMODnet Bathymetry Consortium (2022). EMODnet Digital Bathymetry (DTM 2022).

<https://doi.org/10.12770/ff3aff8a-cff1-44a3-a2c8-1910bf109f85>.

Mooring BB and FF: authors are grateful to the cruise participants who helped us with the mooring servicing, in particular the captain and the crew members of the R/V Urania, R/V Minerva Uno, R/V G. Dallaporta, R/V Laura Bassi, and R/V OGS Explora, as well as the fishing boats Pasquale & Cristina and Attila. The maintenance of the BB and FF fixed moorings over time was only possible due to the support of the following projects: EU - Next Generation EU Mission 4 “Education and Research” - Component 2: “From research to business” - Investment 3.1: “Fund for the realisation of an integrated system of research and innovation infrastructures” - Project IR0000032 – ITINERIS - Italian Integrated Environmental Research Infrastructures System - CUP B53C22002150006; the European Community’s Seventh Framework Programme projects “Hotspot Ecosystem Research and Man’s Impact on European seas” (HERMIONE; grant agreement no. 226354) and “Towards Coast to COast NETworks of marine protected areas (from the shore to the high and deep sea), coupled with sea based wind energy potential” (COCONET; grant agreement no. 287844); RITMARE (Italian Research for the Sea; grant no. SP5_WP3_AZ1) flagship project. The mooring are part of South Adriatic Regional Facility of EMSO-ERIC consortium and is supported by a grant from Istituto Nazionale di Geofisica e Vulcanologia within the framework of the Joint Research EMSO Italia through funds devoted by the Italian Ministry of University and Research to international dimension activities linked to the European Research Infrastructure EMSO and by a grant from the Ufficio Programmazione e Grant Office of CNR-Italy (CNR-UPGO).

The authors express their gratitude to the following projects for providing financial support for the operation of PALOMA station: JERICO-NEXT (Grant Agreement No. 654410), RITMARE (Italian Research for the Sea; Grant No. SP5_WP3), and the Ufficio Programmazione e Grant Office of CNR-Italy (CNR-UPGO).

References

- Barra, E., Riminucci, F., Dinelli, E., Albertazzi, S., Giordano, P., Ravaioli, M., & Capotondi, L. (2020). Natural versus anthropic influence on north adriatic coast detected by geochemical analyses. *Applied Sciences*, 10 (18). <https://doi.org/10.3390/app10186595>
- Benetazzo, A., Bergamasco, A., Bonaldo, D., Falcieri, F., Sclavo, M., Langone, L., & Carniel, S. (2014). Response of the adriatic sea to an intense cold air outbreak: Dense water dynamics and wave-induced transport. *Progress in Oceanography*, 128, 115-138. <https://doi.org/10.1016/j.pocean.2014.08.015>
- Bensi, M., Cardin, V., Rubino, A., Notarstefano, G., & Poulain, P. M. (2013). Effects of winter convection on the deep layer of the southern adriatic sea in 2012. *Journal of Geophysical Research: Oceans*, 118 (11), 6064-6075. <https://doi.org/10.1002/2013JC009432>
- Berta, M., Bellomo, L., Griffo, A., Magaldi, M. G., Molcard, A., Mantovani, C., Gasparini, G. P., Marmain, J., Vetrano, A., Béguery, L., Borghini, M., Barbin, Y., Gaggelli, J., & Quentin, C. (2018). Wind-induced variability in the northern current (northwestern mediterranean sea) as depicted by a multi-platform observing system. *Ocean Science*, 14(4), 689–710. <https://doi.org/10.5194/os-14-689-2018>
- Bignami, F., Salusti, E., & Schiarini, S. (1990). Observations on a bottom vein of dense water in the southern adriatic and ionian seas. *Journal of Geophysical Research: Oceans*, 95 (C5), 7249-7259. <https://doi.org/10.1029/JC095iC05p07249>
- Böhm, E., Riminucci, F., Bortoluzzi, G., Colella, S., Aciri, F., R., S., & Ravaioli, M. (2016). Operational use of continuous surface fluorescence measurements offshore rimini to validate satellite-derived chlorophyll observations. *Journal of Operational Oceanography*, 9 (sup1), s167–s175. <https://doi.org/10.1080/1755876X.2015.1117763>
- Boldrin, A., Carniel, S., Giani, M., Marini, M., Bernardi Aubry, F., Campanelli, A., Grilli, F., & Russo, A. (2009). Effects of bora wind on physical and biogeochemical properties of stratified waters in the northern adriatic. *Journal of Geophysical Research: Oceans*, 114 (C8). <https://doi.org/10.1029/2008JC004837>

Bonaldo, D., Benetazzo, A., Bergamasco, A., Campiani, E., Foglini, F., Sclavo, M., Trincardi, F., & Carniel, S. (2016). Interactions among adriatic continental margin morphology, deep circulation and bedform patterns. *Marine Geology*, 375, 82-98. (Cascading Dense water Flow and its Impact on the Sea Floor in the Adriatic and Aegean Sea, Eastern Mediterranean) <https://doi.org/10.1016/j.margeo.2015.09.012>

Bosse, A., Testor, P., Damien, P., Estournel, C., Marsaleix, P., Mortier, L., Prieur, L., & Taillandier, V. (2021). Wind-forced submesoscale symmetric instability around deep convection in the northwestern mediterranean sea. *Fluids*, 6 (3). <https://doi.org/10.3390/fluids6030123>

Buljan, M., & Zore-Amanda, M. (1966). Hydrographic data on the adriatic sea collected in the period from 1952 through 1964. *Acta Adriatica*, 12, 1–438.

Buongiorno Nardelli, B., Tronconi, C., Pisano, A., & Santoleri, R. (2013). High and ultra high-resolution processing of satellite sea surface temperature data over southern european seas in the framework of myocean project. *Remote Sensing of Environment*, 129, 1-16. <https://doi.org/10.1016/j.rse.2012.10.012>

Cantoni, C., Luchetta, A., Celio, M., Cozzi, S., Raicich, F., & Catalano, G. (2012). Carbonate system variability in the gulf of trieste (north adriatic sea). *Estuarine, Coastal and Shelf Science*, 115, 51-62. (Fluctuations and trends in the northern Adriatic marine systems: from annual to decadal variability) <https://doi.org/10.1016/j.ecss.2012.07.006>

Cardin, V., Wirth, A., Khosravi, M., & Gačić, M. (2020). South adriatic recipes: Estimating the vertical mixing in the deep pit. *Frontiers in Marine Science*, 7. <https://doi.org/10.3389/fmars.2020.565982>

Carniel, S., Bonaldo, D., Benetazzo, A., Bergamasco, A., Boldrin, A., Falcieri, F. M., Sclavo, M., Trincardi, F., & Langone, L. (2016). Off-shelf fluxes across the southern adriatic margin: Factors controlling dense-water-driven transport phenomena. *Marine Geology*, 375, 44-63. (Cascading Dense water Flow and its Impact on the Sea Floor in the Adriatic and Aegean Sea, Eastern Mediterranean) <https://doi.org/10.1016/j.margeo.2015.08.016>

Ceramicola S., Cova A., Forlin E., Markezic N., Mangano G., Civile D., Zecchin ,Fanucci F., Colizza E., Corselli C., Morelli D., Savini A., Caburlotto A., Candoni O., Coste M., Cotterle D., Critelli S., Cuppari A., Deponte M., Dominici M., Facchin L., Gordini E., Locatelli M., Muto F., Praeg D., Romeo R. & Tessarolo, C. (2024). Geohazard Features of the Ionian Calabrian Margin. *Journal of Maps*, 20(1). <https://doi.org/10.1080/17445647.2024.2349785>

Cerino, F., Fornasaro, D., Kralj, M., Giani, M., & Cabrini, M. (2019). Phytoplankton temporal dynamics in the coastal waters of the north-eastern adriatic sea (mediterranean sea) from 2010 to 2017. *Nature Conservation*, 34, 343-372. <https://doi.org/10.3897/natureconservation.34.30720>

Chiggiato, J., Schroeder, K., Moure, B., Miramontes, E., Lionello, P., Marcos, M., Pinardi, N., Mason, E., Álvarez, M., & Trincardi, F. (2023). Chapter 1- introduction. In K. Schroeder & J. Chiggiato (Eds.), *Oceanography of the Mediterranean sea* (p.1-11). Elsevier. <https://doi.org/10.1016/B978-0-12-823692-5.00002-9>

Chiggiato, J., Schroeder, K., & Trincardi, F. (2016). Cascading dense shelf-water during the extremely cold winter of 2012 in the adriatic, mediterranean sea: Formation, flow, and seafloor impact. *Marine Geology*, 375, 1-4. (Cascading Dense water Flow and its Impact on the Sea Floor in the Adriatic and Aegean Sea, Eastern Mediterranean) <https://doi.org/10.1016/j.margeo.2016.03.002>

Coppola, L., Legendre, L., Lefevre, D., Prieur, L., Taillandier, V., & Diamond Riquier, E. (2018). Seasonal and interannual variations of dissolved oxygen in the north-western mediterranean sea (dyfamed site). *Progress in Oceanography*, 162, 187-201. <https://doi.org/10.1016/j.pocean.2018.03.001>

Darmaraki, S., Somot, S., Sevault, F., Nabat, P., Cabos Narvaez, W. D., Cavicchia, L., Djurdjevic, V., Li, L., Sannino, G., & Sein, D. V. (2019). Future evolution of marine heatwaves in the mediterranean sea. *Climate Dynamics*, 53 (3), 1371-1392. <https://doi.org/10.1007/s00382-019-04661-z>

de Boyer Montégut, C., Madec, G., Fischer, A. S., Lazar, A., & Iudicone, D. (2004). Mixed layer depth over the global ocean: An examination of profile data and a profile-based climatology. *Journal of Geophysical Research: Oceans*, 109 (C12). <https://doi.org/10.1029/2004JC002378>

De Santis, A., Chiappini, M., Marinaro, G., Guardato, S., Conversano, F., D'Anna, G., Di Mauro, D., Cardin, V., Carluccio, R., Rende, S. F., Giordano, R., Rossi, L., Simeone, F., Giacomozzi, E., Fertitta, G., Costanza, A., Donnarumma, G., Riccio, R., Siena, G., & Civitarese, G. (2022). Insea project: Initiatives in supporting the consolidation and enhancement of the emso infrastructure and related activities. *Frontiers in Marine Science*, 9. <https://doi.org/10.3389/fmars.2022.846701>

Durrieu de Madron, X., Aubert, D., Charrière, B., Kunesch, S., Menniti, C., Radakovitch, O., & Sola, J. (2023). Impact of dense water formation on the transfer of particles and trace metals from the coast to the deep in the northwestern mediterranean. *Water*, 15 (2). <https://doi.org/10.3390/w15020301>

693 Escudier, R., Clementi, E., Cipollone, A., Pistoia, J., Drudi, M., Grandi, A., Lyubartsev, V., Lecci, R., Aydogdu, A., Delrosso,
694 D., Omar, M., Masina, S., Coppini, G., & Pinardi, N. (2021). A high-resolution reanalysis for the mediterranean sea.
695 *Frontiers in Earth Science*, 9. <https://doi.org/10.3389/feart.2021.702285>

696 Escudier, R., Clementi, E., Omar, M., Cipollone, A., Pistoia, J., Aydogdu, A., Drudi, M., Grandi, A., Lyubartsev, V., Lecci,
697 R., Cret'ı, S., Masina, S., Coppini, G., & Pinardi, N. (2020). *Mediterranean sea physical reanalysis (cmems med-currents)*
698 *(version 1)*. https://doi.org/10.25423/CMCC/MEDSEA_MULTIYEAR_PHY_006_004_E3R1

699 Eusebi Borzelli, G. L., & Carniel, S. (2023). A reconciling vision of the adriatic-ionic bimodal oscillating system.
700 *Scientific Reports*, 13 (1), 2334. <https://doi.org/10.1038/s41598-023-29162-2>

701 Eusebi Borzelli, G. L., Napolitano, E., Carillo, A., Struglia, M. V., Palma, M., & Iacono, R. (2024). Hydrographic vs. dynamic
702 description of a basin: The example of baroclinic motion in the ionic sea. *Oceans*, 5 (2), 383–397.
703 <https://doi.org/10.3390/oceans5020023>

704 Fedele, G., Mauri, E., Notarstefano, G., & Poulain, P. M. (2022). Characterization of the atlantic water and levantine
705 intermediate water in the mediterranean sea using 20 years of argo data. *Ocean Science*, 18 (1), 129–142.
706 <https://doi.org/10.5194/os-18-129-2022>

707 Fourrier, M., Coppola, L., D'Ortenzio, F., Migon, C., & Gattuso, J.-P. (2022). Impact of intermittent convection in the
708 northwestern mediterranean sea on oxygen content, nutrients, and the carbonate system. *Journal of Geophysical*
709 *Research: Oceans*, 127 (9), e2022JC018615. (e2022JC018615 2022JC018615) <https://doi.org/10.1029/2022JC018615>

710 Gačić, M., Civitarese, G., Kovačević, V., Ursella, L., Bensi, M., Menna, M., Cardin, V., Poulain, P.-M., Cosoli, S.,
711 Notarstefano, G., & Pizzi, C. (2014). Extreme winter 2012 in the adriatic: an example of climatic effect on the bios
712 rhythm. *Ocean Science*, 10 (3), 513–522. <https://doi.org/10.5194/os-10-513-2014>

713 Gačić, M., Eusebi Borzelli, G. L., Civitarese, G., Cardin, V., & Yari, S. (2010). Can internal pro- cesses sustain reversals of
714 the ocean upper circulation? the ionic sea example. *Geophysical Research Letters GEOPHYS RES LETT*, 37.
715 <https://doi.org/10.1029/2010GL043216>

716 Gačić, M., Ursella, L., Kovačević, V., Menna, M., Malačić, V., Bensi, M., Negretti, M.-E., Cardin, V., Orlić, M., Sommeria,
717 J., Viana Barreto, R., Viboud, S., Valran, T., Petelin, B., Siena, G., & Rubino, A. (2021). Impact of dense-water flow over
718 a sloping bottom on open-sea circulation: laboratory experiments and an ionic sea (mediterranean) example. *Ocean*
719 *Science*, 17 (4), 975–996. <https://doi.org/10.5194/os-17-975-2021>

720 Grilli, F., Accoroni, S., Acri, F., Bernardi Aubry, F., Bergami, C., Cabrini, M., Campanelli, A., Giani, M., Guicciardi, S., Marini,
721 M., Neri, F., Penna, A., Penna, P., Pugnetti, A., Ravaioli, M., Riminucci, F., Ricci, F., Totti, C., Viaroli, P., & Cozzi, S. (2020).
722 Seasonal and interannual trends of oceanographic parameters over 40 years in the northern adriatic sea in relation to
723 nutrient loadings using the emodnet chemistry data portal. *Water*, 12 (8). <https://doi.org/10.3390/w12082280>

724 Grilli, F., Marini, M., Degobbi, D., Ferrari, C. R., Fornasiero, P., Russo, A., Gismondi, M., Djakovac, T., Precali, R., &
725 Simonetti, R. (2005). Circulation and horizontal fluxes in the northern adriatic sea in the period June 1999-July 2002.
726 part II: nutrients transport. *Sci Total Environ*, 353 (1-3), 115–125. <https://doi.org/10.1016/j.scitotenv.2005.09.011>

727 Hersbach, H., Bell, B., Berrisford, P., Biavati, G., Horányi, A., Muñoz Sabater, J., Nicolas, J., Peubey, C., Radu, R., Rozum,
728 I., Schepers, D., Simmons, A., Soci, C., Dee, D., & Thépaut, J.-N. (2023). Era5 hourly data on single levels from 1940 to
729 present. *Copernicus Climate Change Service (C3S) Climate Data Store (CDS)*. (Accessed on 21-Nov-2024)
730 <https://doi.org/10.24381/cds.adbb2d47>

731 Houpert, L., Durrieu de Madron, X., Testor, P., Bosse, A., D'Ortenzio, F., Bouin, M. N., Dausse, D., Le Goff, H., Kunesch,
732 S., Labaste, M., Coppola, L., Mortier, L., & Raimbault, P. (2016). Observations of open-ocean deep convection in the
733 northwestern mediterranean sea: Seasonal and interannual variability of mixing and deep water masses for the 2007-
734 2013 period. *Journal of Geophysical Research: Oceans*, 121 (11), 8139-8171. <https://doi.org/10.1002/2016JC011857>

735 Ivanov, V., Shapiro, G., Huthnance, J., Aleynik, D., & Golovin, P. (2004). Cascades of dense water around the world ocean.
736 *Progress in Oceanography*, 60 (1), 47-98. <https://doi.org/10.1016/j.pocean.2003.12.002>

737 Janeković, I., Mihanović, H., Vilibić, I., & Tudor, M. (2014). Extreme cooling and dense water formation estimates in open
738 and coastal regions of the adriatic sea during the winter of 2012. *Journal of Geophysical Research: Oceans*, 119 (5),
739 3200-3218. <https://doi.org/10.1002/2014JC009865>

740 Josey, S. A., & Schroeder, K. (2023). Declining winter heat loss threatens continuing ocean convection at a
741 mediterranean dense water formation site. *Environmental Research Letters*, 18 (2), 024005.
742 <https://doi.org/10.1088/1748-9326/aca9e4>

743 Josey, S. A., Somot, S., & Tsimplis, M. (2011). Impacts of atmospheric modes of variability on mediterranean sea surface
744 heat exchange. *Journal of Geophysical Research: Oceans*, 116 (C2). <https://doi.org/10.1029/2010JC006685>

745 Kokkini, Z., Mauri, E., Gerin, R., Poulain, P., Simoncelli, S., & Notarstefano, G. (2020). On the salinity structure in the
746 south adriatic as derived from float and glider observations in 2013–2016. *Deep Sea Research Part II: Topical Studies*
747 *in Oceanography*, 171, 104625. (Revisiting the Eastern Mediterranean: Recent knowledge on the physical,
748 biogeochemical and ecosystemic states and trends (Volume II)) <https://doi.org/10.1016/j.dsr2.2019.07.013>

749 Kovačević, V., Ursella, L., Gačić, M., Notarstefano, G., Menna, M., Bensi, M., & Poulain, P.-M. (2015). On the ionian
750 thermohaline properties and circulation in 2010–2013 as measured by argo floats. *Acta Adriatica*, 56 (1), 97–114.

751 Kubin, E., Menna, M., Mauri, E., Notarstefano, G., Mieruch, S., & Poulain, P.-M. (2023). Heat content and temperature
752 trends in the mediterranean sea as derived from argo float data. *Frontiers in Marine Science*, 10.
753 <https://doi.org/10.3389/fmars.2023.1271638>

754 Kubin, E., Poulain, P.-M., Mauri, E., Menna, M., & Notarstefano, G. (2019). Levantine intermediate and levantine deep
755 water formation: An argo float study from 2001 to 2017. *Water*, 11 (9). <https://doi.org/10.3390/w11091781>

756 Langone, L., Conese, I., Miserocchi, S., Boldrin, A., Bonaldo, D., Carniel, S., Chiggiato, J., Turchetto, M., Borghini, M., &
757 Tesi, T. (2015). Dynamics of particles along the western margin of the southern adriatic: Processes involved in
758 transferring particulate matter to the deep basin. *Marine Geology*, 375. <https://doi.org/10.1016/j.margeo.2015.09.004>

759 Li, M., Organelli, E., Serva, F., Bellacicco, M., Landolfi, A., Pisano, A., Marullo, S., Shen, F., Mignot, A., van Gennip, S., &
760 Santoleri, R. (2024). Phytoplankton spring bloom inhibited by marine heatwaves in the north-western mediterranean
761 sea. *Geophysical Research Letters*, 51 (20), e2024GL109141. (e2024GL109141 2024GL109141)
762 <https://doi.org/10.1029/2024GL109141>

763 Le Meur, J.: PhD Thesis Intermittent supply of dense water to the deep South Adriatic Pit: an observational study.

764 Liu, F., Mikolajewicz, U., & Six, K. D. (2022). Drivers of the decadal variability of the north ionian gyre upper layer
765 circulation during 1910–2010: a regional modelling study. *Climate Dynamics*, 58 (7), 2065–2077.
766 <https://doi.org/10.1007/s00382-021-05714-y>

767 Malanotte Rizzoli and the Pan-Med group et al., (2012). Physical forcing and physical/biochemical variability of the
768 Mediterranean Sea: a review of unresolved issues and directions for future research. *Report of the Workshop*
769 *“Variability of the Eastern and Western Mediterranean circulation and thermohaline properties: similarities and*
770 *differences” Rome 7-9 November 2011*, 48 pp.

771 Malanotte-Rizzoli, P., Artale, V., Borzelli-Eusebi, G. L., Brenner, S., Crise, A., Gačić, M., Kress, N., Marullo, S., Ribera
772 d’Alcalà, M., Sofianos, S., Tanhua, T., Theocharis, A., Alvarez, M., Ashkenazy, Y., Bergamasco, A., Cardin, V., Carniel, S.,
773 Civitarese, G., D’Ortenzio, F., Font, J., Garcia-Ladona, E., Garcia-Lafuente, J. M., Gogou, A., Gregoire, M., Hainbucher, D.,
774 Kontoyannis, H., Kovacevic, V., Kraskapoulou, E., Kroskos, G., Incarbona, A., Mazzocchi, M. G., Orlic, M., Ozsoy, E.,
775 Pascual, A., Poulain, P.-M., Roether, W., Rubino, A., Schroeder, K., Siokou-Frangou, J., Souvermezoglou, E., Sprovieri,
776 M., Tintoré, J., & Triantafyllou, G. (2014). Physical forcing and physical/biochemical variability of the mediterranean sea:
777 a review of unresolved issues and directions for future research. *Ocean Science*, 10 (3), 281–322.
778 <https://doi.org/10.5194/os-10-281-2014>

779 Manca, B., Ibellio, V., Pacciaroni, M., Scarazzato, P., & Giorgetti, A. (2006). Ventilation of deep waters in the adriatic and
780 ionian seas following changes in thermohaline circulation of the eastern mediterranean. *Climate Research - CLIMATE*
781 *RES*, 31, 239–256. <https://doi.org/10.3354/cr031239>

782 Manca, B., Kovačević, V., Gačić, M., & Viezzoli, D. (2002). Dense water formation in the southern adriatic sea and
783 spreading into the ionian sea in the period 1997–1999. *Journal of Marine Systems*, 33–34, 133–154. (MATER: MAss
784 Transfer and Ecosystem Response) [https://doi.org/10.1016/S0924-7963\(02\)00056-8](https://doi.org/10.1016/S0924-7963(02)00056-8)

785 Mantziafou, A., & Lascaratos, A. (2004). An eddy resolving numerical study of the general circulation and deep-water
786 formation in the Adriatic Sea. *Deep Sea Research Part I: Oceanographic Research Papers*, 51(7), 921–952.
787 <https://doi.org/10.1016/j.dsr.2004.03.006>

788 Margirier, F., Testor, P., Heslop, E., Mallil, K., Bosse, A., Houpert, L., Mortier, L., Bouin, M.-N., Coppola, L., D’Ortenzio, F.,
789 Durrieu de Madron, X., Mourre, B., Prieur, L., Raimbault, P., & Taillandier, V. (2020). Abrupt warming and salinification
790 of intermediate waters interplays with decline of deep convection in the northwestern mediterranean sea. *Scientific*
791 *Reports*, 10 (1), 20923. <https://doi.org/10.1038/s41598-020-77859-5>

792 Marini, M., Maselli, V., Campanelli, A., Foglini, F., & Grilli, F. (2016). Role of the mid-adriatic deep in dense water
793 interception and modification. *Marine Geology*, 375, 5–14. (Cascading Dense water Flow and its Impact on the Sea Floor
794 in the Adriatic and Aegean Sea, Eastern Mediterranean) <https://doi.org/10.1016/j.margeo.2015.08.015>

795 Marini, M., Russo, A., Paschini, E., Grilli, F., & Campanelli, A. (2006). Short-term physical and chemical variations in the
796 bottom water of middle adriatic depressions. *Climate Research*, 31 (2–3), 227–237. <https://doi.org/10.3354/cr031227>

797 Marshall, J., & Schott, F. (1999). Open-ocean convection: Observations, theory, and models. *Reviews of Geophysics*, 37
798 (1), 1-64. <https://doi.org/10.1029/98RG02739>

799 Martellucci, R., Menna, M., Mauri, E., Pirro, A., Gerin, R., Paladini de Mendoza, F., Garić, R., Batistić, M., di Biagio, V.,
800 Giordano, P., Langone, L., Miserocchi, S., Gallo, A., Notarstefano, G., Savonitto, G., Bussani, A., Pacciaroni, M., Zuppelli,
801 P., & Poulain, P.-M. (2024). Recent changes of the dissolved oxygen distribution in the deep convection cell of the
802 southern adriatic sea. *Journal of Marine Systems*, 245, 103988. <https://doi.org/10.1016/j.jmarsys.2024.103988>

803 Martellucci, R., Salon, S., Cossarini, G., Piermattei, V., & Marcelli, M. (2021). Coastal phytoplankton bloom dynamics in
804 the tyrrhenian sea: Advantage of integrating in situ observations, large-scale analysis and forecast systems. *Journal of*
805 *Marine Systems*, 218, 103528. <https://doi.org/10.1016/j.jmarsys.2021.103528>

806 Matić-Skoko, S., Pavičić, M., Šepić, J., Janeković, I., Vrdoljak, D., Vilibić, I., Stagličić, N., Šegvić Bubić, T., & Vujević, A.
807 (2022). Impacts of sea bottom temperature on cpue of european lobster homarus gammarus (linnaeus, 1758; decapoda,
808 nephropidae) in the eastern adriatic sea. *Frontiers in Marine Science*, 9. <https://doi.org/10.3389/fmars.2022.891197>

809 Mauri, E., Gerin, R., & Poulain, P.-M. (2016). Measurements of water-mass properties with a glider in the south-western
810 adriatic sea. *Journal of Operational Oceanography*, 9(sup1), s3-s9. <https://doi.org/10.1080/1755876X.2015.1117766>

811 McDougall, T., & Barker, P. (2011). Getting started with teos-10 and the gibbs seawater (gsw)oceanographic toolbox.
812 *SCOR/IAPSO WG*, 127, 1-28.

813 Meli, M. (2024). The potential recording of north ionian gyre's reversals as a decadal signal in sea level during the
814 instrumental period. *Scientific Reports*, 14 (1), 4907. <https://doi.org/10.1038/s41598-024-55579-4>

815 Menna, M., Gačić, M., Martellucci, R., Notarstefano, G., Fedele, G., Mauri, E., Gerin, R., & Poulain, P.-M. (2022). Climatic,
816 decadal, and interannual variability in the upper layer of the mediterranean sea using remotely sensed and in-situ data.
817 *Remote Sensing*, 14 (6). <https://doi.org/10.3390/rs14061322>

818 Menna, M., Gerin, R., Notarstefano, G., Mauri, E., Bussani, A., Pacciaroni, M., & Poulain, P.-M. (2021). On the circulation
819 and thermohaline properties of the eastern Mediterranean Sea. *Frontiers in Marine Science*, 8.
820 <https://doi.org/10.3389/fmars.2021.671469>

821 Menna, M., Suarez, N. C. R., Civitarese, G., Gačić, M., Rubino, A., & Poulain, P. (2019). Decadal variations of circulation
822 in the central mediterranean and its interactions with mesoscale gyres. *Deep Sea Research Part II: Topical Studies in*
823 *Oceanography*. 164, 14-24. <https://doi.org/10.1016/j.dsr2.2019.02.004>

824 Mihanović, H., Vilibić, I., Carniel, S., Tudor, M., Russo, A., Bergamasco, A., Bubić, N., Ljubešić, Z., Viličić, D., Boldrin, A.,
825 Malačić, V., Celio, M., Comici, C., & Raicich, F. (2013). Exceptional dense water formation on the adriatic shelf in the
826 winter of 2012. *Ocean Science*, 9 (3), 561–572. <https://doi.org/10.5194/os-9-561-2013>

827 Mihanović, H., Vilibić, I., Sepić, J., Matić, F., Ljubešić, Z., Mauri, E., Gerin, R., Notarstefano, G., & Poulain, P.-M. (2021).
828 Observation, preconditioning and recurrence of exceptionally high salinities in the adriatic sea. *Frontiers in Marine*
829 *Science*, 8. <https://doi.org/10.3389/fmars.2021.672210>

830 Neri, F., Romagnoli, T., Accoroni, S., Campanelli, A., Marini, M., Grilli, F., & Totti, C. (2022). Phytoplankton and
831 environmental drivers at a long-term offshore station in the northern adriatic sea (1988–2018). *Continental Shelf*
832 *Research*, 242, 104746. <https://doi.org/10.1016/j.csr.2022.104746>

833 Neri, F., Romagnoli, T., Accoroni, S., Ubaldi, M., Garzia, A., Pizzuti, A., Campanelli, A., Grilli, F., Marini, M., & Totti, C.
834 (2023). Phytoplankton communities in a coastal and offshore stations of the northern adriatic sea approached by
835 network analysis and different statistical descriptors. *Estuarine, Coastal and Shelf Science*, 282, 108224.
836 <https://doi.org/10.1016/j.ecss.2023.108224>

837 Nigam, T., Escudier, R., Pistoia, J., Aydogdu, A., Omar, M., Clementi, E., Cipollone, A., Drudi, M., Grandi, A., Mariani, A.,
838 Lyubartsev, V., Lecci, R., Cret'i, S., Masina, S., Coppini, G., & Pinardi, N. (2021). *Mediterranean Sea physical reanalysis*
839 *interim (cmems med-currents, e3r1i system) (version 1)*.
840 https://doi.org/10.25423/CMCC/MEDSEA_MULTIYEAR_PHY_006_E3R1

841 Orlić, M., Dadić, V., Grbec, B., Leder, N., Marki, A., Matić, F., Mihanović, H., Beg Paklar, G., Pasarić, M., Pasarić, Z., &
842 Vilibić, I. (2006). Wintertime buoyancy forcing, changing seawater properties, and two different circulation systems
843 produced in the adriatic. *Journal of Geophysical Research: Oceans*, 111 (C3). <https://doi.org/10.1029/2005JC003271>

844 Paladini de Mendoza, F., Schroeder, K., Miserocchi, S., Borghini, M., Giordano, P., Chiggiato, J., Trincardi, F., Amorosi,
845 A., & Langone, L. (2023a). Sediment resuspension and transport processes during dense water cascading events along
846 the continental margin of the southern adriatic sea (mediterranean sea). *Marine Geology*, 459, 107030.
847 <https://doi.org/10.1016/j.margeo.2023.107030>

848 Paladini de Mendoza, F., Schroeder, K., Langone, L., Chiggiato, J., Borghini, M., Giordano, P., & et al. (2022). Deep-
849 water hydrodynamic observations of two moorings sites on the continental slope of the southern adriatic sea
850 (mediterranean sea). *Earth System Science Data*, 14 (12), 5617–5635. <https://doi.org/10.5194/essd-14-5617-2022>

851 Paladini de Mendoza, F., Schroeder, K., Langone, L., Chiggiato, J., Borghini, M., Giordano, P., & Miserochi, S. (2023b).
852 Deep-water dynamics along the 2012–2020 observations on the continental margin of the southern adriatic sea
853 (mediterranean sea). *Journal of Marine Science and Engineering*, 11(7). <https://doi.org/10.3390/jmse11071364>

854 Parras-Berrocal, I. M., Vázquez, R., Cabos, W., Sein, D. V., Álvarez, O., Bruno, M., & Izquierdo, (2023). Dense water
855 formation in the eastern mediterranean under a global warming scenario. *Ocean Science*, 19 (3), 941–952.
856 <https://doi.org/10.5194/os-19-941-2023>

857 Parras-Berrocal, I. M., Vázquez, R., Cabos, W., Sein, D. V., Álvarez, O., Bruno, M., & Izquierdo, A. (2022). Surface and
858 intermediate water changes triggering the future collapse of deep water formation in the north western
859 mediterranean. *Geophysical Research Letters*, 49 (4), e2021GL095404. (e2021GL095404 2021GL095404)
860 <https://doi.org/10.1029/2021GL095404>

861 Pastor, F., Valiente, J. A., & Khodayar, S. (2020). A warming mediterranean: 38 years of increasing sea surface
862 temperature. *Remote Sensing*, 12 (17). <https://doi.org/10.3390/rs12172687>

863 Pinardi, N., Cessi, P., Borile, F., & Wolfe, C. L. P. (2019). The mediterranean sea overturning circulation. *Journal of*
864 *Physical Oceanography*, 49 (7), 1699 - 1721. <https://doi.org/10.1175/JPO-D-18-0254.1>

865 Pinardi, N., Estournel, C., Cessi, P., Escudier, R., & Lyubartsev, V. (2023). Chapter 7 -dense and deep water formation
866 processes and mediterranean overturning circulation. In K. Schroeder & J. Chiggiato (Eds.), *Oceanography of the*
867 *Mediterranean sea* (p.209-261). Elsevier. <https://doi.org/10.1016/B978-0-12-823692-5.00009-1>

868 Pirro, A., Mauri, E., Gerin, R., Martellucci, R., Zuppelli, P., & Poulain, P. M. (2022). New insights on the formation and
869 breaking mechanism of convective cyclonic cones in the south adriatic pit during winter 2018. *Journal of Physical*
870 *Oceanography*, 52 (9), 2049-2068. <https://doi.org/10.1175/JPO-D-21-0108.1>

871 Pirro, A., Martellucci, R., Mauri, E., Menna M. (2022). New insights on the formation and breaking mechanism of
872 convective cyclonic cones in the south adriatic pit during winter 2018. *Journal of Physical Oceanography*, 52 (9), 2049-
873 2068. <https://doi.org/10.1175/JPO-D-21-0108.1>

874 Pirro, A., Martellucci, R., Gallo, A., Kubin, E., Mauri, E., Juza, M., Notarstefano G., Pacciaroni M., Bussani A., Menna, M.
875 (2024). Subsurface warming derived from Argo floats during the 2022 Mediterranean marine heat wave. *of the*
876 *Copernicus Ocean State Report (OSR8)*, edited by: von Schuckmann, K., Moreira, L., Grégoire, M., Marcos, M., Staneva,
877 J., Brasseur, P., Garric, G., Lionello, P., Karstensen, J., and Neukermans, G., *Copernicus Publications, State Planet*.

878 Pranić, P., Denamiel, C., & Vilibić, I. (2021). Performance of the adriatic sea and coast (adrisc) climate component – a
879 coawst v3.3-based one-way coupled atmosphere–ocean modelling suite: ocean results. *Geoscientific Model*
880 *Development*, 14 (10), 5927–5955. <https://doi.org/10.5194/gmd-14-5927-2021>

881 Querin, S., Bensi, M., Cardin, V., Solidoro, C., Bacer, S., Mariotti, L., Stel, F., & Malacic, V. (2016). Saw-tooth modulation
882 of the deep water thermohaline properties in the southern Adriatic sea. *Journal of Geophysical Research: Oceans*, 121.
883 <https://doi.org/10.1002/2015JC011522>

884 Raicich F., Malačić V., Celio M., Giaiotti D., Cantoni C., Colucci R.R., Čermelj B., and Pucillo A. (2013). Extreme Air-Sea
885 Interactions in the Gulf of Trieste (North Adriatic) during the strong Bora event in winter 2012. *Journal of Geophysical*
886 *Research: Oceans*, 118, 5238 – 5250. <https://doi:10.1002/jgrc.20398>

887 Ravaioli, M., Bergami, C., Riminucci, F., Langone, L., Cardin, V., Di Sarra, A., Aracri, S., Bastianini, M., Bensi, M.,
888 Bergamasco, A., Bommarito, C., Borghini, M., Bortoluzzi, G., Bozzano, R., Cantoni, C., Chiggiato, J., Crisafi, E., D’Adamo,
889 R., Durante, S., Fanara, C., Grilli, F., Lipizer, M., Marini, M., Miserochi, S., Paschini, E., Penna, P., Pensieri, S., Pugnetti,
890 A., Raicich, F., Schroeder, K., Siena, G., Specchiulli, A., Stanghellini, G., Vetrano, A., & Crise, A. (2016). The ritmare italian
891 fixed-point observatory network (ifon) for marine environmental monitoring: a case study. *Journal of Operational*
892 *Oceanography*, 9 (sup1), s202–s214. <https://doi.org/10.1080/1755876X.2015.1114806>

893 Reale, M., Cossarini, G., Lazzari, P., Lovato, T., Bolzon, G., Masina, S., Solidoro, C., & Salon, S. (2022). Acidification,
894 deoxygenation, and nutrient and biomass declines in a warming mediterranean sea. *Biogeosciences*, 19 (17), 4035–
895 4065. <https://doi.org/10.5194/bg-19-4035-2022>

896 Reale, M., Crise, A., Farneti, R., & Mosetti, R. (2016). A process study of the adriatic-ionian system baroclinic dynamics.
897 *Journal of Geophysical Research: Oceans*, 121, 5872–5887. <https://doi.org/10.1002/2016JC011763>

898 Reale, M., Salon, S., Crise, A., Farneti, R., Mosetti, R., & Sannino, G. (2017). Unexpected covariant behavior of the
899 aegean and ionian seas in the period 1987–2008 by means of a nondimensional sea surface height index. *Journal of*
900 *Geophysical Research: Oceans*, 122 (10), 8020-8033. <https://doi.org/10.1002/2017JC012983>

901 Reale, M., Salon, S., Somot, S., Solidoro, C., Giorgi, F., Crise, A., Cossarini, G., Lazzari, P., & Sevault, F. (2020). Influence
 902 of large-scale atmospheric circulation patterns on nutrient dynamics in the mediterranean sea in the extended winter
 903 season (october-march) 1961- 1999. *Climate Research*, 82. <https://doi.org/10.3354/cr01620>
 904 Rétif, S., Negretti, M. E., & Wirth, A. (2024). Predicting the vertical density structure of oceanic gravity current intrusions.
 905 *Scientific Reports*, 14(1), 10274.

906 Rio, M.-H., Pascual, A., Poulain, P.-M., Menna, M., Barceló, B., & Tintoré, J. (2014). Computation of a new mean dynamic
 907 topography for the mediterranean sea from model outputs, altimeter measurements and oceanographic in situ data.
 908 *Ocean Science*, 10 (4), 731–744. <https://doi.org/10.5194/os-10-731-2014>
 909 Rovere, M., Pellegrini, C., Chiggiato, J., Campiani, E., & Trincardi, F. (2019). Impact of dense bottom water on a
 910 continental shelf: An example from the sw adriatic margin. *Marine Geology*, 408, 123-143.
 911 <https://doi.org/10.1016/j.margeo.2018.12.002>
 912 Rubino, A., Gačić, M., Bensi, M., Kovačević, V., Malačič, V., Menna, M., Negretti, M. E., Sommeria, J., Zanchettin, D.,
 913 Barreto, R. V., Ursella, L., Cardin, V., Civitarese, G., Orlić, M., Petelin, B., & Siena, G. (2020). Experimental evidence of
 914 long-term oceanic circulation reversals without wind influence in the north ionian sea. *Sci Rep*, 10 (1), 1905.
 915 <https://doi.org/10.1038/s41598-020-57862-6>
 916 Rubino, A., Romanenkov, D., Zanchettin, D., Cardin, V., Hainbucher, D., Bensi, M., Boldrin, A., Langone, L., Miserocchi,
 917 S., & Turchetto, M. (2012). On the descent of dense water on a complex canyon system in the southern adriatic basin.
 918 *Continental Shelf Research*, 44, 20-29. (Southern Adriatic Oceanography) <https://doi.org/10.1016/j.csr.2010.11.009>
 919 Sellschopp, J., & Álvarez, A. (2003). Dense low-salinity outflow from the adriatic sea under mild (2001) and strong
 920 (1999) winter conditions. *Journal of Geophysical Research*, 108. <https://doi.org/10.1029/2002JC001562>
 921 Shapiro, G. I., Huthnance, J. M., & Ivanov, V. V. (2003). Dense water cascading off the continental shelf. *Journal of*
 922 *Geophysical Research: Oceans*, 108 (C12). <https://doi.org/10.1029/2002JC001610>
 923 Somot, S., Houpert, L., Sevault, F., Testor, P., Bosse, A., Taupier-Letage, I., Bouin, M.-N., Waldman, R., Cassou, C.,
 924 Sanchez-Gomez, E., Durrieu de Madron, X., Adloff, F., Nabat, P., & Herrmann, M. (2018). Characterizing, modelling and
 925 understanding the climate variability of the deep water formation in the north-western mediterranean sea. *Climate*
 926 *Dynamics*, 51 (3), 1179-1210. <https://doi.org/10.1007/s00382-016-3295-0>
 927 Schroeder, K., Ben Ismail, S., Bensi, M., Bosse, A., Chiggiato, J., Civitarese, G., Falcieri, M., Fusco, G., Gačić, M.,
 928 Gertman, I., Kubin, E., Malanotte-Rizzoli, P., Martellucci, R., Menna, M., Ozer, T., Taupier-Letage, I., Vargas-Yáñez, M.,
 929 Velaoras, D., & Vilibić, I. (2024). A consensus-based, revised and comprehensive catalogue for Mediterranean water
 930 masses acronyms. *Mediterranean Marine Science*, 25(3), 783–791. <https://doi.org/10.12681/mms.38736>
 931 Tassigny, A., Negretti, M. E., & Wirth, A. (2024). Dynamics of intrusion in downslope gravity currents in a rotating frame.
 932 *Physical Review Fluids*, 9(7), 074605.

933 Testor, P., Bosse, A., Houpert, L., Margirier, F., Mortier, L., Legoff, H., Dausse, D., Labaste, M., Karstensen, J., Hayes, D.,
 934 Olita, A., Ribotti, A., Schroeder, K., Chiggiato, J., Onken, R., Heslop, E., Mourre, B., D'ortenzio, F., Mayot, N., Lavigne,
 935 H., de Fommervault, O., Coppola, L., Prieur, L., Taillandier, V., Durrieu de Madron, X., Bourrin, F., Many, G., Damien, P.,
 936 Estournel, C., Marsaleix, P., Taupier-Letage, I., Raimbault, P., Waldman, R., Bouin, M.-N., Giordani, H., Caniaux, G.,
 937 Somot, S., Ducrocq, V., & Conan, P. (2018). Multiscale observations of deep convection in the northwestern
 938 mediterranean sea during winter 2012–2013 using multiple platforms. *Journal of Geophysical Research: Oceans*, 123
 939 (3), 1745-1776. <https://doi.org/10.1002/2016JC012671>
 940 Trincardi, F., Verdicchio, G., & Miserocchi, S. (2007). Seafloor evidence for the interaction between cascading and
 941 along-slope bottom water masses. *Journal of Geophysical Research*, 112. <https://doi.org/10.1029/2006JF000620>
 942 Turchetto, M., Boldrin, A., Langone, L., Miserocchi, S., Tesi, T., & Foglini, F. (2007). Particle transport in the bari canyon
 943 (southern adriatic sea). *Marine Geology*, 246 (2), 231-247. (EUROSTRATAFORM: Role and functioning of Canyons)
 944 <https://doi.org/10.1016/j.margeo.2007.02.007>
 945 Ursella, L., Gačić, M., Kovačević, V., & Deponte, D. (2012). Low-frequency flow in the bottom layer of the strait of
 946 Otranto. *Continental Shelf Research*, 44, 5-19. (Southern Adriatic Oceanography)
 947 <https://doi.org/10.1016/j.csr.2011.04.014>
 948 Vilibić, I., & Mihanović, H. (2013). Observing the bottom density current over a shelf using an argo profiling float.
 949 *Geophysical Research Letters*, 40 (5), 910-915. <https://doi.org/10.1002/grl.50215>
 950 Vilibić, I., Pranić, P., & Denamiel, C. (2023). North adriatic dense water: lessons learned since the pioneering work of
 951 mira zore-armanda 60 years ago.

Vilibić, I., & Supić, N. (2005). Dense water generation on a shelf: The case of the adriatic sea. *Ocean Dynamics*, 55, 403-415. <https://doi.org/10.1007/s10236-005-0030-5>

Waldman, R., Brüggemann, N., Bosse, A., Spall, M., Somot, S., & Sevault, F. (2018). Overturning the Mediterranean thermohaline circulation. *Geophysical Research Letters*, 45 (16), 8407-8415. <https://doi.org/10.1029/2018GL078502>

Wong, A. P. S., Wijffels, S. E., Riser, S. C., Pouliquen, S., Hosoda, S., Roemmich, D., Gilson, J., Johnson, G. C., Martini, K., Murphy, D. J., Scanderbeg, M., Bhaskar, T. V. S. U., Buck, J. J. H., Merceur, F., Carval, T., Maze, G., Cabanes, C., André, X., Poffa, N., Yashayaev, I., Barker, P. M., Guinehut, S., Belbéoch, M., Ignaszewski, M., Baringer, M. O., Schmid, C., Lyman, J. M., McTaggart, K. E., Purkey, S. G., Zilberman, N., Alkire, M. B., Swift, D., Owens, W. B., Jayne, S. R., Hersh, C., Robbins, P., West-Mack, D., Bahr, F., Yoshida, S., Sutton, P. J. H., Cancouët, R., Coatanoan, C., Dobbler, D., Juan, A. G., Gourrion, J., Kolodziejczyk, N., Bernard, V., Bourlès, B., Claustre, H., D'Ortenzio, F., Le Reste, S., Le Traon, P.-Y., Rannou, J.-P., Saout-Grit, C., Speich, S., Thierry, V., Verbrugge, N., Angel-Benavides, I. M., Klein, B., Notarstefano, G., Poulain, P.-M., Vélez-Belchi, P., Suga, T., Ando, K., Iwasaka, N., Kobayashi, T., Masuda, S., Oka, E., Sato, K., Nakamura, T., Sato, K., Takatsuki, Y., Yoshida, T., Cowley, R., Lovell, J. L., Oke, P. R., van Wijk, E. M., Carse, F., Donnelly, M., Gould, W. J., Gowers, K., King, B. A., Loch, S. G., Mowat, M., Turton, J., Rama Rao, E. P., Ravichandran, M., Freeland, H. J., Gaboury, I., Gilbert, D., Greenan, B. J. W., Ouellet, M., Ross, T., Tran, A., Dong, M., Liu, Z., Xu, J., Kang, K., . . . Park, H.-M. (2020). Argo data 1999–2019: Two million temperature-salinity profiles and subsurface velocity observations from a global array of profiling floats. *Frontiers in Marine Science*, 7 . <https://doi.org/10.3389/fmars.2020.00700>

Yari, S., Kovačević, V., Cardin, V., Gačić, M., & Bryden, H. L. (2012). Direct estimate of water, heat, and salt transport through the strait of Otranto. *Journal of Geophysical Research: Oceans*, 117(C9). <https://doi.org/10.1029/2012JC007936>

Zore-Armanda, M. (1963). Les masses d'eau de la mer adriatique. *Acta Adriatica*, 10, 5-88.